University of São Paulo
"Luiz de Queiroz" College of Agriculture

Enzymatic modes of action on soybean hulls and corn distiller's dried grains with solubles considering substrates' structures and variabilities

Diogo Filipe Rosso

Thesis presented to obtain the degree of Doctor in Science. Area: Bioenergy

Piracicaba
2022

Diogo Filipe Rosso
Bioprocess Engineer and Biotechnologist

Enzymatic modes of action on soybean hulls and corn distiller's dried grains with solubles considering substrates' structures and variabilities

Advisor:
Dr. **CARLOS EDUARDO DRIEMEIER**

Thesis presented to obtain the degree of Doctor in Science. Area: Bioenergy

Piracicaba
2022

Dados Internacionais de Catalogação na Publicação
DIVISÃO DE BIBLIOTECA – DIBD/ESALQ/USP

Rosso, Diogo Filipe

Enzymatic modes of action on soybean hulls and corn distiller's dried grains with solubles considering substrates' structures and variabilities / Diogo Filipe Rosso. - - Piracicaba, 2022.

69 p.

Tese (Doutorado) - - USP / Escola Superior de Agricultura "Luiz de Queiroz". Universidade Estadual de Campinas. Universidade Estadual Paulista "Julio de Mesquita Filho"

1. Casca de soja 2. DDGS 3. Variabilidade 4. Valorização 5. Enzima I. Título

ACKNOWLEDGEMENTS

I would firstly like to thank my Ph.D. supervisor, Dr. Carlos Eduardo Driemeier, for his invaluable guidance. His expertise, encouragement, and continuous support were essential for me to mature as a researcher and develop this Thesis. I also would like to acknowledge my mentors Dr. Morten Broch Tovborg and Dr. Roberto Nobuyuki Maeda for the valuable discussions throughout the development of this project.

The journey into the Ph.D. program in Bioenergy would not have started without Viviane Serpa Müller and Victor Guadalupe Medina, and support from Anna Horn, Katrine Pontoppidan, and Lone Nilsson. My special regards to them and all the current and former scientists from the Research and Development departments at Novozymes Latin America (Andrea, Daniel, Eduardo, Kelly, and Michelle) and Novozymes Denmark (Lærke, Mads, Tine, Eduardo, and Ninfa) for their trust in the first steps of this journey.

A special thanks to my colleagues in the lab João, Ana Letícia, Bruna, Camila, Leticia, Emanuelly, Gerson, Matheus, Thiago, Berit, Pernille, and Peter, for their willingness to collaborate and share their experiences and time.

I also thank the team from CNPEM Djanira Negrão, Liu Ling, and Otavio Berenguel for their scientific support on electron microscopy, microtomography, and Raman microspectroscopy techniques and all the technicians for their support.

A very special thanks to my Novozymes team members Jacqueline Chimilovski de Souza and Fernanda Frantz. Their comprehension and friendship were crucial to helping me keep my focus during challenging times.

My sincere gratitude to my family, my parents Pedro and Sílvia, my brother Tiago and sister Alessandra. Despite challenges during my Ph.D. years, including the difficult times during the Covid pandemic, they were there understanding, cheering, and believing in my potential. Last not least, thanks to my cousins Lucas, Daniela, Gabriela, Rafaela, and the others, and all my friends for their encouragement and distraction.

For you all, thank you!

EPIGRAPH

It's ready when you are,
That's pretty unique.

But it won't be easy,
The paper says the forecast will be bumpy and painful,
Lots of rainstorms, heartaches.

But that's life,
Or so I'm told.

When you're ready,
Just walk on through.

The Guardian of Forever

CONTENTS

RESUMO 7
ABSTRACT 8
FIGURES LIST 9
TABLE LIST 11
1. THESIS STRUCTURE 13
2. INTRODUCTION 15
2.1. The industrial importance of soybean and soybean hulls 16
2.2. Perspectives on DDGS production from the corn-ethanol industry 18
References 20
3. OBJECTIVES 23
3.1. Specific objectives 23
4. UNVEILING THE VARIABILITY AND MULTISCALE STRUCTURE OF SOYBEAN HULLS FOR BIOTECHNOLOGICAL VALORIZATION 25
Abstract 25
4.1. Introduction 25
4.2. Material and Methods 27
4.2.1. Collection of SBH samples 27
4.2.2. Compositional analysis 27
4.2.3. Multimodal imaging 28
4.2.4. X-ray diffraction (XRD) 29
4.2.5. Dynamic vapor sorption (DVS) 29
4.2.6. Calorimetric thermoporometry (CTP) 29
4.2.7. Enzymatic hydrolysis 30
4.3. Results and Discussion 30
4.3.1. Visual and compositional variability 30
4.3.2. Tisse-scale structure 35
4.3.3. Cellulose crystallites 38
4.3.4. Hydration 40
4.3.5. Enzymatic hydrolysis 41
4.4. Conclusions 43
References 43

5. VARIABILITY OF SOUTH AMERICAN CORN DISTILLER'S DRIED GRAINS WITH SOLUBLES AND CONSEQUENCES FOR ENZYMATIC UPGRADING 49
Abstract 49
5.1. Introduction 49
5.2. Materials and Methods 51
5.2.1. Collection of the DDGS samples 51
5.2.2. Preparation of extracted DDGS and model substrates 51
5.2.3. Compositional analysis 52
5.2.4. Enzymatic hydrolysis 53
5.2.5. Statistical analysis 53
5.3. Results and Discussion 54
5.3.1. Variability of as-received DDGS 54
5.3.2. Detailing variability through the analysis of extracted DDGS and model substrates .. 57
5.3.3. Enzymatic hydrolysis 60
5.4. Conclusions 65
References 65

RESUMO

Modos de ação enzimática em cascas de soja e grãos de milho destilados secos com solúveis considerando as estruturas e variabilidades dos substratos

A valorização de resíduos agroindustriais através de processos enzimáticos é atrativa uma vez que essas matérias-primas possuem baixo custo, estão disponíveis em plantas industriais, e podem, potencialmente, ter sinergias com a produção de alimentos. Resíduos agroindustriais têm sido estudados para diferentes aplicações, como na produção de químicos biorrenováveis e como ingredientes alternativos na produção animal. No entanto, as suas complexas estruturas de carboidratos estruturais (celulose, hemicelulose, pectina e outros) representam uma barreira para uma valorização eficiente. Nessa Tese, cascas de soja e grãos de milho destilados secos com solúveis (DDGS), subprodutos do processamento industrial da soja e do milho, respectivamente, são investigados devido à sua importância no cenário Sul-americano e seu potencial de valorização. Para ambos, as investigações abrangem a variabilidade composicional, as estruturas dos substratos, e reações enzimáticas, porém a ênfase das investigações é adaptada de acordo com as especificidades de cada substrato. Os estudos sobre a casca de soja concentraram-se no entendimento da estrutura hierárquica multi-escala nativa do substrato, a qual é preservada após a separação industrial das cascas. A casca de soja foi previamente considerada um substrato com alta suscetibilidade à conversão enzimática, o que favorece uma bioconversão sem pré-tratamentos termoquímicos. Essa possibilidade é confirmada nessa Tese. As características multi-escalas contribuem para a compreensão das origens estruturais da baixa recalcitrância da casca de soja. Em meio aquoso, a casca de soja tem alta porosidade em nanoescala, especialmente para tamanhos de poros maiores que tamanhos de enzimas ~ 5mm. Além disso, teores de lignina são baixos e localizados, e a relativa pureza da celulose na estrutura da casca de soja também contribuem para a sua baixa recalcitrância em comparação com outras matérias-primas lignocelulósicas. Esses resultados fornecem uma base estrutural para compreender a baixa recalcitrância, possibilitando assim a criação de novas rotas de valorização biotecnológica da casca de soja. Por sua vez, o DDGS de milho é obtido a partir do processo de produção de etanol de milho e é composto, principalmente, pela fração não digerida dos grãos. Estudos conduzidos em regiões produtoras de etanol de milho, principalmente os Estados Unidos, demonstram que a variabilidade é um fator determinante para a valorização do DDGS. Com o surgimento da indústria de etanol de milho na América do Sul, a variabilidade do DDGS nesta região torna-se uma questão oportuna. Essa Tese investiga amostras de DDGS obtidas de plantas de processamento localizadas no Brasil, Paraguai e Argentina para a avaliação da variabilidade do DDGS na América do Sul e sua relação com hidrólise enzimática. As amostras investigadas apresentaram maior variabilidade composicional em comparação com dados reportados anteriormente em outras regiões. O teor de levedura em DDGS mostrou ser um fator de baixo impacto na variabilidade, enquanto o teor de extrativos e a proporção entre fibra de milho e proteína são os principais fatores de impacto. A hidrólise enzimática com coquetéis otimizados para a lignocelulose, a fibra de milho e a estrutura de leveduras demonstrou efeitos complementares e sinérgicos para a solubilização de componentes estruturais do DDGS em um conjunto de amostras pré-extraídas com alta variabilidade. Além disso, a resposta aos coquetéis enzimáticos pode ser correlacionada com as principais variações de composição do DDGS, estabelecendo dessa forma bases para estratégias de valorização do DDGS considerando seus padrões de variabilidade. Com esses resultados, essa Tese contribui com o estabelecimento de uma base de conhecimentos robusta para o desenvolvimento de estratégias de valorização para cascas de soja e DDGS de milho através de rotas enzimáticas.

Palavras-chave: Casca de soja, DDGS, Variabilidade, Valorização, Enzima

ABSTRACT

Enzymatic modes of action on soybean hulls and corn distiller's dried grains with solubles considering substrates' structures and variabilities

Valorization of agroindustrial residues through enzymatic upgrading is attractive because such feedstocks are inexpensive, available at industrial sites, and potentially synergistic with the production of food. Agroindustrial residues have been studied for applications such as the production of bio-renewable chemicals and alternative ingredients in animal production. However, their complex structural polysaccharides (cellulose, hemicelluloses, pectins, and others) represent a barrier to efficient valorization. In this Thesis, soybean hulls (SBH) and corn distiller's dried grains with solubles (DDGS), by-products of the industrial processing of soybean and corn, respectively, are investigated because of their importance in the South American landscape and the potential for valorization. For both types of substrates, the investigation covers compositional variability, substrate structure, and enzymatic reactions, but the emphasis of the investigation is tailored to the specificities of each type of substrate. The investigation of SBH privileged the understanding of the native hierarchical multiscale structure of the biomass, which is mostly preserved after the industrial separation of the hulls. SBH has been previously recognized as a substrate highly amenable to enzymatic conversion (*i.e.*, low recalcitrance), which allows bioconversion without thermochemical pretreatment. This possibility is confirmed by this work. The multiscale characteristics of SBH shed light on the structural origins of the low recalcitrance. In aqueous media SBH have high nanoscale porosity, especially for pore sizes greater than enzyme sizes ~5mm. Moreover, the contents of lignin are low and localized, and the relative purity of cellulose in SBH tissues also contributes to the low recalcitrance of SBH compared to other lignocellulosic feedstocks. These results provide a structural basis for understanding the low recalcitrance of SBH, paving the way for novel developments in SBH biotechnological valorization. As corn DDGS is concerned, this biomass is obtained from the corn ethanol production process and is composed mainly of the undigested fraction of corn grains. The experience from traditional production regions, chiefly the United States, has shown that variability is a key factor for DDGS valorization. With the emergence of the corn ethanol industry in South America, the variability of DDGS in this new production region becomes a timely question. This work investigates DDGS samples obtained by facilities from Brazil, Paraguay, and Argentina to learn about the variability of DDGS in South America and the consequences for enzymatic hydrolysis. The investigated samples presented higher compositional variability in comparison to previously reported data from other production regions. Yeast content in DDGS is shown to be a minor factor contributing to variability, whereas the content of extractives and the proportion between corn fiber and protein are major ones. Enzymatic hydrolysis with cocktails optimized for lignocellulose, corn fiber, and yeast revealed complementary and synergistic effects for the solubilization of DDGS structural components in a highly variable set of pre-extracted DDGS. Furthermore, the response to enzymes could be correlated to the main compositional variations of DDGS, establishing a basis for enzymatic strategies to upgrade DDGS with consideration of its patterns of variability. With these results, this Thesis contributes to the advancement of a robust knowledge base for the development of enzymatic upgrading strategies for SBH and corn DDGS.

Keywords: Soybean hulls, DDGS, Variability, Valorization, Enzyme

FIGURES LIST

Figure 1. Flowchart of soybean industrial processing through solvent extraction. 17

Figure 2. Flowchart representing a dry-mill bioethanol production process19..... 19

Figure 3. Visualization of the soybean hull samples. Note the different colors, particle sizes, and aggregation states: (SA-SE) loose hulls and (SF-SH) pelletized hulls 31

Figure 4. Principal component analysis of the soybean hull composition matrix. (a) Scores discriminating samples (SA-SH). (b) Loadings discriminating the relations between compositional attributes. GalA – Insoluble galacturonan, Glc -Insoluble glucan, Ara – Insoluble arabinan, Xyl – Insoluble xylan, Gal – Insoluble galactan, Man – Insoluble mannan, Lig – Insoluble Lignin, Ex(W&E) – Water-Ethanol extractives, Ex(Hex) – n-Hexane extractives, Prot – Insoluble Protein..... 33

Figure 5. Visualization of soybean hull structures at the tissue scale. a – Hilum and extrahilar region: two main specialized structures in soybean seed; b – SEM image of a selected cross-section in which yellow arrows show depressions in the outermost layer of SBH; c – Three-dimensional rendered reconstruction of an SBH fragment imaged by μCT; d,e,f – orthogonal visualizations from μCT, in which yellow arrows show cracks in the internal structure of SBH. The orthogonal visualizations were obtained from the same point indicated at intersections of the yellow lines. Major extrahilar hull tissues are indicated. PL – palisade layers, HL – hourglass layer; PA – parenchyma..... 36

Figure 6. Polarized Raman spectra from (a) palisade cells and (b) hourglass cells using vertical and horizontal laser polarization. Location and polarization of the laser are indicated in the inset images .. 37

Figure 7. Raman spectra from soybean hull tracheid bar..... 38

Figure 8. X-ray diffraction from SBH and comparison with parameters obtained from sugarcane bagasse. (a) SBH experimental, calculated, and residual (experimental–calculated) two-dimensional diffraction patterns are presented at the top, middle, and bottom, respectively. (b) Example of SBH diffractogram (η=0°). Experimental (blue line) and calculated (red line) intensities presented with contributions from the background (black line) and individual diffraction peaks (dotted gray lines). Circles identify positions from all cellulose Iβ diffraction peaks. (c) Crystal width L200 determined from SBH compared to sugarcane bagasse. (d) Comparison of diffractograms obtained from SBH and sugarcane bagasse. 39

Figure 9. Vapor sorption isotherm (left) and thermoporometry profiles (right) of selected SBH samples. Sugarcane samples are included as a comparative lignocellulosic biomass with higher lignin contents. 41

Figure 10. Yield (wt.%) of solubilized fraction, glucose (Glc), and xylose (Xyl) after submitting soybean hulls to enzymatic hydrolysis. 42

Figure 11. Visualization of the as-received corn DDGS samples (SA-SI). Note variations in color and particle size. 54

Figure 12. Principal component analysis of the as-received corn DDGS composition matrix. (A) Scores discriminating samples (SA-SH). (B) Loadings discriminating the relations between compositional attributes. Glc -Insoluble glucan, Ara – Insoluble arabinan, Xyl – Insoluble xylan, Gal – Insoluble galactan, Man – Insoluble mannan, AIR – Acid insoluble residue, Ex(W&E) – Water-Ethanol extractives, Ex(Hex) – n-Hexane extractives, Prot – Insoluble Protein..... 56

Figure 13. Principal component analysis of the composition matrix of the extracted DDGS and model substrates. (A) Scores discriminating samples (eSA, eSC, eSE, eSI, de-starched corn, and inactivated yeast). (B) Loadings discriminating the relations between compositional attributes. Glc -Insoluble glucan, Ara – Insoluble arabinan, Xyl – Insoluble xylan, Gal – Insoluble galactan, Man – Insoluble mannan, AIR – Acid insoluble residue, Prot – Insoluble Protein.....59

Figure 14. Principal component analysis of enzymatic hydrolysis responses from extracted DDGS and extracted model substrates. (A) Scores discriminating samples by symbols (eSA: +, eSC: x, eSE: z, eSI: *, de-starched corn: ■, inactivated yeast: ▲) and treatments by color (Control – black, LC: green, CF: red; YF: Blue, Combination: Purple). (B) Loadings discriminating the relations between analyzed responses. Tot Mass – Solubilized total mass (wt.%), Prot – Solubilized protein (wt.%), Glc -Solubilized glucose (wt.%), Ara – Solubilized arabinose (wt.%), Xyl – Solubilized xylose (wt.%), Gal – Solubilized galactose (wt.%), Man – Solubilized mannose (wt.%).....62

Figure 15. Principal component analysis of enzymatic hydrolysis responses from extracted DDGS and extracted de-starched corn. (A) Scores discriminating samples by symbols (eSA: +, eSC: x, eSE: z, eSI: *, de-starched corn: ■) and treatments by color (Control – black, LC: green, CF: red; YF: Blue, Combination: purple). (B) Loadings discriminating the relations between analyzed responses. Tot Mass – Solubilized mass (wt.%), Prot – Solubilized protein (wt.%), Glc -Solubilized glucose (wt.%), Ara – Solubilized arabinose (wt.%), Xyl – Solubilized xylose (wt.%), Gal – Solubilized galactose (wt.%), Man – Solubilized mannose (wt.%).....63

Figure 16. Correlation matrix between compositional components of extracted substrates (columns) and response to enzymatic treatments (rows).....64

TABLE LIST

Table 1. Composition of Soybean Feed Ingredient Products (wt.%)12 17

Table 2. Composition of soybean hulls given as wt.% of dry matter. 32

Table 3. Composition of as-received corn DDGS given as wt.% dry matter 55

Table 4. Composition of the selected samples of extracted DDGS and model substrates given as wt.% dry matter. 57

Table 5. Results of enzymatic hydrolysis 61

1. THESIS STRUCTURE

This Thesis document presents an introduction, the objectives of the doctoral project, and two main chapters formatted as research articles. The first article is already published (Rosso, D.F., Negrão, D.R. & Driemeier, C. Unveiling the Variability and Multiscale Structure of Soybean Hulls for Biotechnological Valorization. Waste Biomass Valor 13, 2095–2108 (2022). https://doi.org/10.1007/s12649-021-01655-z). The second article is still pending submission for publication.

The introduction chapter presents the potential of agroindustrial residues as inexpensive renewable feedstocks that can be upgraded using enzymatic treatments. The two feedstocks evaluated in this Thesis, soybean hulls (SBH) and corn distiller's dried grain with solubles (DDGS), are presented with a contextualization of the importance of these materials in the South American landscape.

The chapter "UNVEILING THE VARIABILITY AND MULTISCALE STRUCTURE OF SOYBEAN HULLS FOR BIOTECHNOLOGICAL VALORIZATION" comprises the published learnings generated for soybean hulls. Multimodal analysis (electron microscopy, X-ray microtomography, Raman spectromicroscopy, X-ray diffraction, dynamic vapor sorption, calorimetric thermoporometry, and enzymatic hydrolysis) have been employed to investigate SBH variability and the relation between the multiscale structure and the high enzymatic digestibility of this lignocellulosic biomass. The obtained results provide a structural basis for understanding the low recalcitrance of SBH, paving the way for novel developments in SBH biotechnological valorization.

The chapter entitled "VARIABILITY OF SOUTH AMERICAN CORN DISTILLER'S DRIED GRAINS WITH SOLUBLES AND CONSEQUENCES FOR ENZYMATIC UPGRADING" presents an investigation of the compositional variability of South American DDGS and its impact on enzymatic hydrolysis. Enzymatic cocktails targeting lignocellulosic biomass, corn fiber, and yeast fermentation were employed to demonstrate complementarity and synergy. The obtained results establish a basis for enzymatic strategies to upgrade DDGS with consideration of its patterns of variability.

2. INTRODUCTION

Agroindustrial residues are recognized as second-generation feedstocks due to their potential use as alternatives to food crops (first-generation feedstocks), as well as their higher availability and lower price[1]. The potential of the residues has been largely studied for a variety of applications, such as the production of value-added bio-renewable chemicals, and as alternative raw materials in animal feed ingredients.

The main challenges with using these lignocellulosic biomasses are related to their complex structural polysaccharide composition and the efficient conversion of this structure into simple sugar monomers[1]. In these plant-derived materials, the complex chemical compounds comprise mostly structural polysaccharides of cell walls and lignin. The structural components are non-starch polysaccharides (NSP), which comprise cellulose, hemicelluloses, pectins, and other less studied polysaccharides. NSP comprises a complex group of carbohydrates typically characterized by long polymeric chains, containing several linked monomeric units of glucose, xylose, and other pentose and hexose monosaccharides[2]. Due to high complexity, different criteria have been used to classify these carbohydrates, such as the methodology of extraction and isolation proposed by Neukom in 1976[3], or classification in three main groups: cellulose, non-cellulosic polymers, and pectic polysaccharides, proposed by Bailey in 1973[4] and based on their monomeric residues and chemical linkage.

The variability of NSP contributes to important differences in composition and concentration within different substrates. While total-NSP represents approximately 10 wt.% (dry-matter) of corn, corn distiller's dried grains with solubles (DDGS) contain approximately 30 wt.%[5], and soybean meal approximately 20 wt.% of total NSP[6,7]. Due to these differences in composition and concentration, efficient conversion to their monomers requires detailed knowledge of the structure and enzymatic mode of action.

The conversion of NSP into simple monosaccharides can be achieved with multiple enzyme activities such as cellulases, hemicellulases, and pectinases. Such enzymes impact the solubilization of cell walls, as well as other constituents like storage polysaccharides (*e.g.*, starch). Consequently, the availability of simple sugars for further transformation into fuels and chemicals or its use as an additional energy source for animal feed[8] is enhanced.

Several feedstocks rich in NSP are available in Brazil and have the potential for different commercial applications. Among these feedstocks, we highlight soybean hulls (SBH) and corn DDGS, by-products of the soy and corn industrial processing, respectively. Soybeans are the major protein source produced in Brazil with reported production of 138 million tonnes between

2020/2021[9], with SBH representing around 7-8 wt.% of this crop. As corn processing is concerned, the first exclusive first-generation corn ethanol production plant was inaugurated in Brazil in August 2017 with a capacity of 240 million liters of ethanol annually. Currently, both SBH and corn DDGS are used as feed ingredients but have limitations due to their composition which results in low nutrient availability.

2.1. The industrial importance of soybean and soybean hulls

Soybeans, due to their high protein and oil content, are one of the main crops in the world. The oil fraction has applications as an ingredient within human and animal nutrition, as well as in biodiesel production and the cosmetics industry[10]. Soybean protein is a high-content and highly digestible protein product commonly used as livestock feed ingredient as well as human food.

In the process of removing the oil fraction from soybeans and obtaining protein, soybean hulls are generated. This residue, which accounts for 7-8 % of the total mass of the crop, is often considered a waste of soybean processing[11].

Different processes have been described for the processing of soybeans, such as screw pressing, extruding/expelling process, and, the most commonly used, solvent extraction[12]. These processes aim at obtaining a more protein-rich product as well as soybean oil and differ in the method used for oil extraction. The solvent-extraction (Figure 1) is the most widely used process, with more than 99 % of the United States capacity using it.

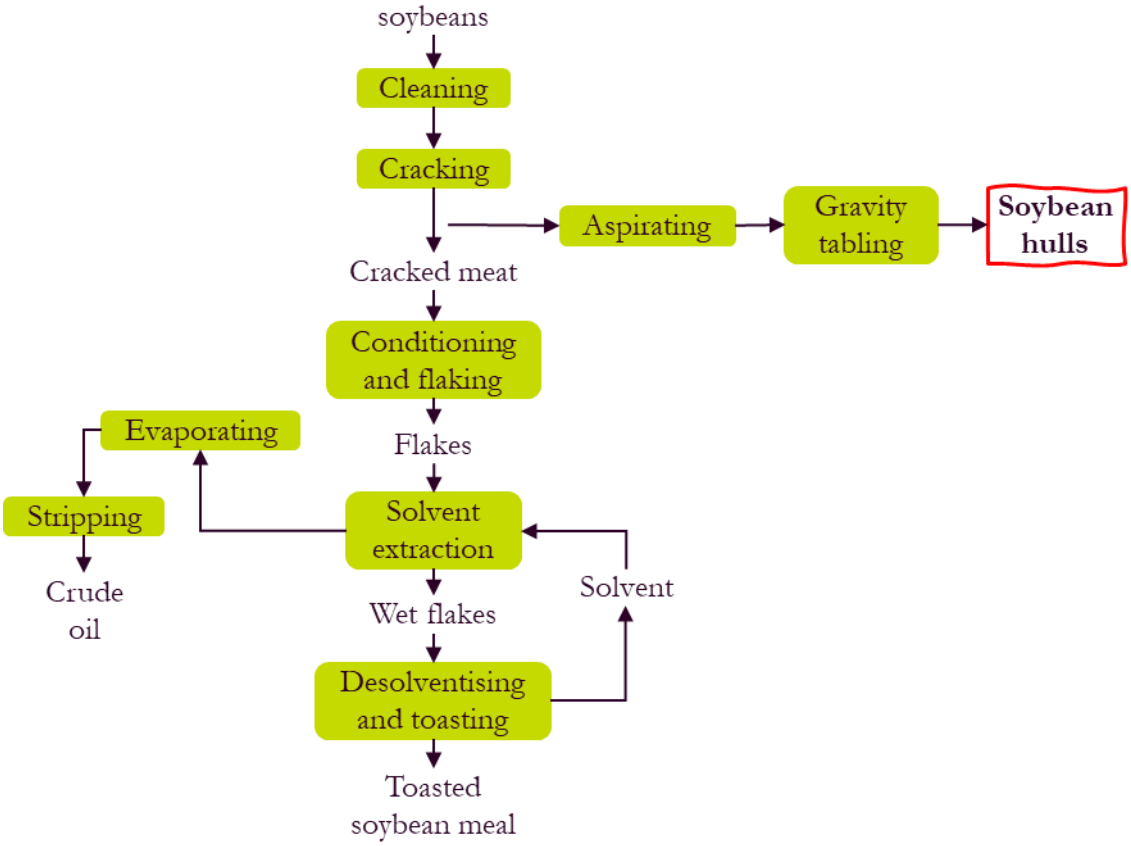

Figure 1. Flowchart of soybean industrial processing through solvent extraction.

SBH are obtained after the first two steps of the process, cleaning and cracking of the soybeans. The following steps of conditioning, flaking and expanding aim at increasing the extraction yields, which results in a de-oiled material, as well as in crude oil[12].

SBH finds limited applications for animal feeding[13] whereas soybean meal dominates the global feed market for vegetable protein meals[14]. The limited use of SBH is caused by the high amounts of non-starch polysaccharides, which attracts large amounts of water and consequently depresses the digestion of fats, saccharides, and proteins[15]. Table 1 shows the comparative composition of soybean, soybean meal, and soybean hulls.

Table 1. Composition of Soybean Feed Ingredient Products (wt.%)[12]

	Soybean	Soybean meal (dehulled, solvent-extracted)	Soybean hulls
Dry-matter	90	88	91
Crude Protein	38	47.8	12.1
Crude Fiber	5	3	40.1

The high fiber content of SBH, however, also demonstrates the high potential of this by-product. The application of NSP-degrading enzymes is well-acknowledged today[16], which can reduce the water holding capacity of the material, and therefore may have a positive influence on nutrient absorption. Mielenz *et* al. (2009) also studied the conversion of the carbohydrates in soybean hulls to ethanol and stated that significant quantities of this biofuel could be obtained[7]. Besides ethanol, an added-value product with increased protein content and reduced fiber content could be obtained.

The world annual production of soybean is estimated at 336 million tons, with 119 million tons produced in Brazil[17]. It is predicted that there will be 29.7–37.1 million tons of soybean hulls available by 2030[18], which confirms the potential use of this by-product for different applications in biofuels and animal feed.

2.2. Perspectives on DDGS production from the corn-ethanol industry

Distiller's Dried Grains with Solubles (DDGS) are the major co-product of the dry-grind production of bioethanol from cereal grains, such as corn[5]. Corn DDGS is obtained after the fermentation of corn starch. DDGS is composed mainly of the remaining, non-fermentable fraction from the corn grain. The dry-grind bioethanol production process from corn starch is shown schematically in Figure 2.

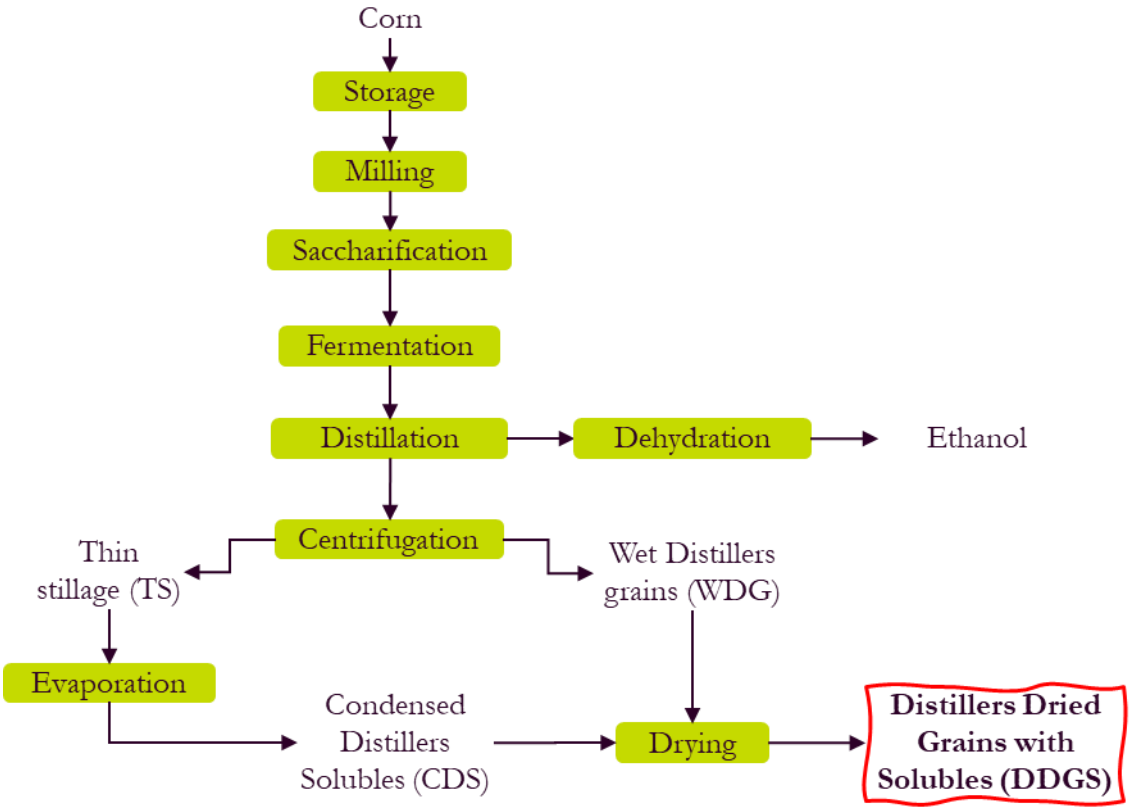

Figure 2. Flowchart representing a dry-mill bioethanol production process[19].

After milling, corn is mixed with enzymes for the saccharification process, in which starch is hydrolyzed into fermentable sugars. These sugars are fermented by the yeast, converting them into ethanol and carbon dioxide. The ethanol is recovered by distillation and dehydration, while the non-volatile fraction is centrifuged to separate the liquid fraction, called thin stillage, and the solid fraction, called wet distiller's grain (WDG). An evaporation step is responsible for concentrating the liquid fraction and producing the condensed distillers soluble (CDS), which is mixed with the WDG and drum dried at high temperatures to produce the final DDGS.

In 2017, approximately 59 million m^3 of ethanol have been produced in the United States, around 85 % produced from the corn dry-milling process. Approximately 40 million tons of distiller's grains were generated[20]. This number has been steadily increasing since around the year 2000 when 7.6 million m^3 of ethanol were produced[21]. Brazil, on the other hand, is currently using a new model of distillery/flex plant, where saccharine (sugarcane) and starch (corn) raw materials are processed in the same industrial site[22].

Besides the flex plants, the first ethanol production plant in Brazil that uses exclusively corn as raw material was inaugurated in August 2017. Five months after its inauguration, the FS Bioenergia group announced the duplication of the first plant and the plans for the construction

of the second production plant, with a combined production capacity of 1.2 billion liters of ethanol, 900 thousand tonnes of corn meal, and 35 thousand tonnes of oil every year[23].

As the production of corn ethanol grows, the amounts of co-products from the biorefineries also increase. Considering the expected increase of traditional co-products output from the expanding corn-to-ethanol biorefineries, it is critical to identify and develop new value-added co-products that will open up new markets for fermentation byproducts[24].

Currently, DDGS is mainly used as cattle feed and is used at low inclusion levels in poultry and swine diets because of its high fiber content[25]. NSP makes up 25–30 wt.% of the DDGS, with the two major components of the NSP being arabinoxylan and cellulose[24]. Although NSP degrading enzymes have already been used in different studies to investigate their effects on nutrient digestibility of DDGS, further investigations are still necessary to elucidate the effect of these enzymes on DDGS hydrolysis and nutrient release for non-ruminant animals[25].

References

(1) Bardhan, S. K.; Gupta, S.; Gorman, M. E.; Haider, M. A. Biorenewable Chemicals: Feedstocks, Technologies and the Conflict with Food Production. Renewable and Sustainable Energy Reviews 2015, 51, 506–520. https://doi.org/10.1016/j.rser.2015.06.013.

(2) Sinha, A. K.; Kumar, V.; Makkar, H. P. S.; De Boeck, G.; Becker, K. Non-Starch Polysaccharides and Their Role in Fish Nutrition – A Review. Food Chemistry 2011, 127 (4), 1409–1426. https://doi.org/10.1016/j.foodchem.2011.02.042.

(3) Neukon, H. Chemistry and Properties of the Non-Starchy Polysaccharides (NSP) of Wheat Flou. LWT Lebensmitt Wissensch Technol 1976, 9, 6.

(4) Bailey, R. W. Structural Carbohydrates. In Chemistry and Biochemistry of Herbage; Academic Press: London, UK, 1973; Vol. 1, pp 157–206.

(5) Pedersen, M. B.; Dalsgaard, S.; Knudsen, K. E. B.; Yu, S.; Lærke, H. N. Compositional Profile and Variation of Distillers Dried Grains with Solubles from Various Origins with Focus on Non-Starch Polysaccharides. Animal Feed Science and Technology 2014, 197, 130–141. https://doi.org/10.1016/j.anifeedsci.2014.07.011.

(6) Al Loman, A.; Ju, L.-K. Enzyme-Based Processing of Soybean Carbohydrate: Recent Developments and Future Prospects. Enzyme and Microbial Technology 2017, 106, 35–47. https://doi.org/10.1016/j.enzmictec.2017.06.013.

(7) Mielenz, J. R.; Bardsley, J. S.; Wyman, C. E. Fermentation of Soybean Hulls to Ethanol While Preserving Protein Value. Bioresource Technology 2009, 100 (14), 3532–3539. https://doi.org/10.1016/j.biortech.2009.02.044.

(8) Pedersen, N. R.; Ravn, J. L.; Pettersson, D. A Multienzyme NSP Product Solubilises and Degrades NSP Structures in Canola and Mediates Protein Solubilisation and Degradation in Vitro. Animal Feed Science and Technology 2017, 234, 244–252. https://doi.org/10.1016/j.anifeedsci.2017.09.015.

(9) CONAB, Companhia Nacional de Abastecimento. Boletim Da Safra de Grãos; 10o Levantamento-Safra 2021/22; Companhia Nacional do Abastecimento, 2022.

(10) Liu, H.-M.; Li, H.-Y. Application and Conversion of Soybean Hulls. In Soybean - The Basis of Yield, Biomass and Productivity; Kasai, M., Ed.; InTech, 2017. https://doi.org/10.5772/66744.

(11) Ferrer, A.; Salas, C.; Rojas, O. J. Physical, Thermal, Chemical and Rheological Characterization of Cellulosic Microfibrils and Microparticles Produced from Soybean Hulls. Industrial Crops and Products 2016, 84, 337–343. https://doi.org/10.1016/j.indcrop.2016.02.014.
(12) Johnson, L.; Smith, K. Soybean Processing; Fact Sheet; Soymeal.org, 2018.
(13) Cortivo, P. R. D.; Hickert, L. R.; Hector, R.; Ayub, M. A. Z. Fermentation of Oat and Soybean Hull Hydrolysates into Ethanol and Xylitol by Recombinant Industrial Strains of Saccharomyces Cerevisiae under Diverse Oxygen Environments. Industrial Crops and Products 2018, 113, 10–18. https://doi.org/10.1016/j.indcrop.2018.01.010.
(14) Friedman, M.; Brandon, D. L. Nutritional and Health Benefits of Soy Proteins. J. Agric. Food Chem. 2001, 49 (3), 1069–1086. https://doi.org/10.1021/jf0009246.
(15) Gulati, H. K.; Chadha, B. S.; Saini, H. S. Production of Feed Enzymes (Phytase and Plant Cell Wall Hydrolyzing Enzymes) ByMucor Indicus MTCC 6333: Purification and Characterization of Phytase. Folia Microbiol 2007, 52 (5), 491–497. https://doi.org/10.1007/BF02932109.
(16) Ravn, J. L.; Martens, H. J.; Pettersson, D.; Pedersen, N. R. Enzymatic Solubilisation and Degradation of Soybean Fibre Demonstrated by Viscosity, Fibre Analysis and Microscopy. JAS 2015, 7 (9), p1. https://doi.org/10.5539/jas.v7n9p1.
(17) USDA. World Agricultural Supply and Demand Estimates; WASDE-599; 2020.
(18) Masuda, T.; Goldsmith, P. D. World Soybean Production: Area Harvested, Yield, and Long-Term Projections. International Food and Agribusiness Management Review 2009, 12 (4), 143–161.
(19) Chatzifragkou, A.; Kosik, O.; Prabhakumari, P. C.; Lovegrove, A.; Frazier, R. A.; Shewry, P. R.; Charalampopoulos, D. Biorefinery Strategies for Upgrading Distillers' Dried Grains with Solubles (DDGS). Process Biochemistry 2015, 50 (12), 2194–2207. https://doi.org/10.1016/j.procbio.2015.09.005.
(20) Renewable Fuels Association. Ethanol Strong - 2018 Ethanol Industry Outlook; 2018; p 34.
(21) Johnston, D. J.; Moreau, R. A. A Comparison between Corn and Grain Sorghum Fermentation Rates, Distillers Dried Grains with Solubles Composition, and Lipid Profiles. Bioresource Technology 2017, 226, 118–124. https://doi.org/10.1016/j.biortech.2016.12.001.
(22) Eckert, C. T.; Frigo, E. P.; Albrecht, L. P.; Albrecht, A. J. P.; Christ, D.; Santos, W. G.; Berkembrock, E.; Egewarth, V. A. Maize Ethanol Production in Brazil: Characteristics and Perspectives. Renewable and Sustainable Energy Reviews 2018, 82, 3907–3912. https://doi.org/10.1016/j.rser.2017.10.082.
(23) FS Bioenergia. FS Bioenergia Announces Mato Grosso´s Second Corn-Only Ethanol Plant Implementation; 2018.
(24) Kim, Y.; Mosier, N. S.; Hendrickson, R.; Ezeji, T.; Blaschek, H.; Dien, B.; Cotta, M.; Dale, B.; Ladisch, M. R. Composition of Corn Dry-Grind Ethanol by-Products: DDGS, Wet Cake, and Thin Stillage. Bioresource Technology 2008, 99 (12), 5165–5176. https://doi.org/10.1016/j.biortech.2007.09.028.
(25) Pedersen, M. B.; Dalsgaard, S.; Arent, S.; Lorentsen, R.; Knudsen, K. E. B.; Yu, S.; Lærke, H. N. Xylanase and Protease Increase Solubilization of Non-Starch Polysaccharides and Nutrient Release of Corn- and Wheat Distillers Dried Grains with Solubles. Biochemical Engineering Journal 2015, 98, 99–106. https://doi.org/10.1016/j.bej.2015.02.036.

3. OBJECTIVES

The general objective of the study is to advance the understanding of the modes of action of different enzyme cocktails on soybean hulls and corn distiller's dried grains with solubles considering the structural characteristics and the variability of the substrates.

3.1. Specific objectives

The study also has the following specific objectives:

- To determine the compositional variability of soybean hulls collected from several facilities in Brazil.
- To determine the level of the recalcitrance of soybean hulls to enzymatic hydrolysis by employing a set of complementary enzyme activities.
- To rationalize the structural origins of the low recalcitrance of soybean hulls by employing multi-modal analysis (electron microscopy, X-ray microtomography, Raman spectromicroscopy, X-ray diffraction, dynamic vapor sorption, and calorimetric thermoporometry).
- To understand the compositional variability of corn DDGS obtained from several facilities in South America.
- To evaluate the impacts of corn DDGS variability on enzymatic hydrolysis by employing a set of complementary enzyme cocktails (optimized for lignocellulose, corn fiber, and yeast cell walls) targeting the main structural components of DDGS.

4. UNVEILING THE VARIABILITY AND MULTISCALE STRUCTURE OF SOYBEAN HULLS FOR BIOTECHNOLOGICAL VALORIZATION

Abstract

Soybean hulls (SBH) are an important agroindustrial residue that is highly susceptible to cellulolytic enzymatic digestion. The multiscale structure of this biomass should be able to inform the origins of its digestibility, but such relationships are currently unknown. This work employs multimodal techniques to learn SBH variability and multiscale structure. Tissue-scale images obtained by electron microscopy, X-ray microtomography, and Raman spectromicroscopy reveal tissue ruptures, lignin localized in the hilum region, and oriented, quite pure cellulose in palisade and hourglass cells of the extra-hilar region. Such specificities of SBH cellulose are reinforced by X-ray diffraction showing cellulose crystallites ~20 % wider than in typical lignocellulosic biomass. SBH are also remarkably more porous than other lignocellulosic feedstocks in the critical pore size (>~10 nm) for enzyme accessibility. Enzymatic hydrolysis confirmed the low recalcitrance of SBH, demonstrating high yields (e.g., 80 % glucose) without SBH pretreatment. These results provide a basis for rationalizing the low recalcitrance of SBH, paving the way for novel developments in SBH biotechnological valorization.

4.1. Introduction

Agroindustrial residues have been recognized as valuable renewable feedstocks due to their low prices, availability, and synergisms with the food supply chain. Here we highlight soybean hulls (SBH), which are residues from the processing of soy (*Glycine max* (L) Merrill) to obtain the protein-rich meal, the oil, and secondary products [1]. World soybean production is about 340-350 million tons per year[2,3] with Brazil and United States jointly accounting for ≈70 % of the production[3]. SBH correspond to 6-8 % of the soybean mass[4,5], from which we calculate a global availability of 20-28 million tons of SBH per year. From a biological perspective, SBH have roles as a mechanical barrier and modulation of interactions between the bean's internal and external environments[6,7], such as water imbibition and protection during germination[8]. From the chemical composition perspective, SBH are made mainly of cellulose, hemiceluloses, and protein, while pectins, fat, lignin, and inorganics are reported as minor components[4,9,10]. At present, SBH are often used as an ingredient in ruminant feed due to their protein, fat, and fiber value. However, large amounts of SBH are still left to waste[9,11,12]. These are low-value uses or even environmental liabilities, creating opportunities for more sophisticated SBH valorization.

In recent years, several new products and conversion pathways have been proposed to valorize SBH. Due to SBH high cellulose contents, transformation into cellulose pulps, derivatives such as carboxymethyl cellulose, hybrid films based on cellulosic microfibrils and microparticles[13], and cellulose nanofibers with high reinforcement potential[14,15] have been

reported. Additionally, SBH have been successfully transformed into biochar applicable as an amendment and carbon sequestration in soils[16], as well as high surface area, activated charcoal[17]. In the area of health and food, SBH were transformed into gel beads applied as a controlled bioactive delivery system[18], and in animal feed studied to evaluate the effect of fiber components on the gastrointestinal microbiome aiming at improving fibrous materials utilization efficiency[19]. Moreover, biotechnological valorization of SBH have considered the potential for carbohydrate hydrolysis, producing soluble sugars fermentable into biofuels and biochemicals[10,12,20]. Previous studies demonstrated that SBH are naturally more digestible than other lignocellulosic feedstocks such as corn stover and wheat straw[10,21,22]. Notably, one study indicated SBH can be converted at high yields in a simultaneous saccharification and fermentation process, without the need for a thermochemical pretreatment step before biochemical conversion[21]. Although this result would position SBH into a select group of cellulosic substrates with natural low recalcitrance, a recent review article on SBH valorization[23] still discusses different pretreatments methods applicable to SBH aiming at maximizing the yield of fermentable products with a low generation of inhibitors. This discussion shows that the potential of SBH for direct digestion (i.e., without pretreatment) by biotechnological processes is still a matter of controversy.

Aiming at understanding the structural origins of SBH digestibility, it is key to first recognize that the characteristics of agroindustrial residues result from the interplay of plant biology and agroindustrial processing. Plant biomass is organized in hierarchical multiscale structures, from molecules to whole organisms, with the key interplay between the distinct length scales of the structural organization[24,25]. These biogenic structures are partly contaminated, degraded, and disrupted by agroindustrial processing[26–28]. Consequently, the resulting variability and multiscale structure of agroindustrial residues can only be fully appreciated with consideration of the interplays between length scales and between biology and agroindustrial processing. In this work, we bring this perspective to investigate the origins of SBH digestibility, employing multimodal analysis to investigate SBH variability, multiscale structure, and enzymatic digestibility. The obtained results provide novel insights for the design of biotechnological processes for the valorization of this renewable feedstock.

4.2. Material and Methods

4.2.1. Collection of SBH samples

Eight SBH samples were kindly provided by five distinct soybean processing facilities in Brazil. The facilities are located in four states (Rio Grande do Sul, Santa Catarina, Paraná, and Minas Gerais) of Brazilian south and southeast regions and therefore span a significant geographic space. Moreover, the SBH sample set includes loose hulls as blown from the beans after crushing as well as pelletized hulls as commercialized by the facilities.

4.2.2. Compositional analysis

Representative aliquots of the SBH samples were dried in a Heratherm oven (Thermo Fisher Scientific, Massachusetts, USA) at 45 °C for 3 h and micronized with a knife-mill (MA048, Marconi, Brazil) using 1 mm output control screen [29]. Ash content was determined by calcination at 575 °C[30]. Protein content was determined with 200 mg aliquots by the Dumas combustion method for crude protein using a nitrogen analyzer (FP-628, Leco Corporation, St. Joseph, MI, USA)[31]. Conversion of nitrogen to protein used a mass conversion factor of 6.25 and ethylenediaminetetra-acetic acid (EDTA) as the nitrogen standard. Contents of extractives were determined by a three-step extraction in an automated system (Dionex Accelerated Solvent Extractor 350, Thermo Fisher Scientific, Massachusetts, USA) using n-hexane, followed by water and ethanol[32]. Oils and fats are expected as n-hexane extractives, while other non-structural components such as sugars, nitrogenous compounds and waxes are expected as water-ethanol extractives.

Extracted samples were submitted to a two-step acid hydrolysis for the determination of structural carbohydrates and lignin. Aliquots of 300 mg of SBH were weighed in triplicates and incubated with 72 % sulfuric acid for 1h at 30 °C. The acid was subsequently diluted to 4 % by adding 84 mL of deionized water and the samples were autoclaved for 1h at 121 °C. Hydrolysates were then vacuum filtered and stored for further analysis[33]. The filtrate was analyzed using high-performance liquid chromatography (HPLC). Monosaccharides (glucose, xylose, arabinose, galactose, mannose, and galacturonic acid) were quantified by HPLC (1200 Infinity, Agilent, Santa Clara, USA) with an Aminex HPX-87P column (300mm x 7.8mm) and a Microguard CarboP guard-column (Bio-Rad Laboratories, Hercules, USA). Glucan, xylan, arabinan, galactan, mannan, and galacturonan were calculated from the concentration of the corresponding monomeric sugars using anhydrous stoichiometric corrections: 0.88 (132/150) for C-5 sugars

(xylose and arabinose), 0.90 (162/180) for C-6 sugars (glucose, galactose, and mannose), and 0.91 (176/194) for galacturonic acid. Insoluble lignin was determined gravimetrically as the remaining residue after the two-step acid hydrolysis corrected for acid-insoluble ash[33]. Mass closure was calculated as the summation of n-hexane extractives, water-ethanol extractives, insoluble protein, insoluble lignin, polymeric sugars, and ashes.

The matrix of compositional data was analyzed by principal components analysis (PCA) using the statistical package SAS JMP 14, to indicate possible clustering between distinct attributes (chemical components) and distinct SBH samples.

4.2.3. Multimodal imaging

X-ray computed microtomography (μCT) was performed at the IMX beamline of the Brazilian Synchrotron Light Laboratory (LNLS)[28] aiming at providing non-invasive 3D visualization of the internal structure of SBH. In this technique, 3D images were acquired with air-dried particles of SBH stick on a stub without any additional sample preparation. The sample was rotated around the vertical axis to acquire 1001 projection images, which were then converted to 3D reconstructed images with voxel size of (0.82 μm)^3. The 3D images were processed with the Fiji/ImageJ[34] software to produce cross-sections and rendered visualizations.

For additional imaging studies, SBH samples were fixed in 4 % formaldehyde in PBS solution (0.2 M Na_2HPO_4, 0.2 M NaH_2PO_4 in pH 7.2) during 6 days at 4 °C, and then transferred in crescent sucrose solutions[35] (10 %, 15 %, 20 %, 24 h each concentration). After that, samples were gradually immersed in OCT (Tissue-Tek Optimal Cutting Temperature, Allkgel, Alkimia Brazil)[36] containing 20 % sucrose (1:1), for 3 days, and then transferred to OCT for 10 days at 4 °C to allow complete infiltration of the polymer. Samples were frozen in liquid nitrogen and stored at -80 °C. Before the cross-sectioning, samples were brought into a Cryostat chamber (Leica 3050 Cryostat, Leica Biosystems, Buffalo Grove, IL, United States) at -25 °C for 4 h[35]. The 70 μm thickness cross sections were collected on glass slides which were immersed in PBS buffer at 4 °C overnight and gently collected and oriented on clean glass slides (22 x 44 mm) and covered with a thin glass slide (2 mm x 2mm), or mounted on Al stubs using stereo stereoscopy (Zeiss Stereo Discover 2.0, Oberkochen, Germany), and stored in a silica desiccator chamber[36].

The sectioned samples on Al stubs were carbon coated and imaged with scanning electron microscopy (SEM). SEM was carried out with a JSM-6610 LV SEM (Jeol USA, Peabody, MA, United States) at the secondary electrons mode, under an accelerating voltage of 10 kV using the low vacuum mode.

For Raman spectromicroscopy (μRaman), samples on glass slides were wet by the addition of water drops. Polarized Raman spectra and associated confocal images were obtained with a XploRA PLUS Raman spectrometer and an Olympus BX40 confocal microscope (Horiba, Kyoto, Japan) using a 638 nm laser, 1200 lines/mm grating, 50× magnification lens, and samples saturated with water covered by a glass coverslip.

4.2.4. X-ray diffraction (XRD)

X-rays were generated by an ultraX-18HF rotating anode generator (Rigaku, Tokyo, Japan) with Cu Kα source (λ=1.5418 Å) and Varimax HR monochromating optics. Milled SBH were filled inside capillary tubes, which were positioned perpendicular to the X-ray beam. Area-detector diffraction patterns were collected in transmission mode by mar345 image plate (Marresearch GmbH, Germany). The Cellulose Rietveld Analysis for Fine Structure (CRAFS) model[37] was used to analyze the diffraction patterns with fixed peak shape parameters as described previously[38].

4.2.5. Dynamic vapor sorption (DVS)

SBH samples were conditioned by exhaustive washing with deionized water. Then, sequential steps of decreasing (desorption) and increasing (sorption) relative humidity at 50 °C were applied by a Q5000 SA dynamic vapor sorption (DVS) instrument (TA Instruments, United States), which measures the sample weight change due to moisture loss or uptake. Desorption and sorption isotherms were created based on the moisture contents measured at the end of each relative humidity step[39].

4.2.6. Calorimetric thermoporometry (CTP)

A differential scanning calorimeter (DSC) Q200 (TA Instruments, United States) was employed for calorimetric thermoporometry (CTP). SBH samples were conditioned by exhaustively washing with deionized water before inserting the wet samples into the DSC pans. In the DSC instrument, the wet samples were frozen to -70 °C and then submitted to sequential heating steps, composed of heating ramps (1 °C/min) and equilibration isotherms. Heat flow thermograms were analyzed to determine the contents of Freezing Bound Water (FBW), corresponding to water with depressed ice melting temperatures due to confinement in

nanometric pores. FBW is presented as cumulative pore size distributions in the range of 1-200 nm expressed as FBW mass per unit of sample dry mass[39].

4.2.7. Enzymatic hydrolysis

SBH were submitted to enzymatic hydrolysis in triplicate in 50 mL tubes, 10 % total solids contents, at pH 5.0, 50 °C for 72h. Sodium acetate buffer (100 mM) was used for pH control and an incubator (Fine PCR COMBI-D24) for temperature control and agitation. Commercial enzyme cocktails Cellic® Ctec3 HS, Viscozyme® L, and Pectinex® Ultra SP-L (Novozymes A/S, Denmark) were used in combination, dosed against dry substrate following manufacturer's activity units (74.7 BHU-2-HS/gSBH, 3 FBG/gSBH, and 99 PGNU/gSBH, respectively). After incubation, each sample was filtered, dried, and insoluble solids were weighed gravimetrically. The solubilized fraction was determined by subtraction. Supernatants were used for sugar determination and quantification of carbohydrate yield after enzymatic hydrolysis.

4.3. Results and Discussion

4.3.1. Visual and compositional variability

Visual inspection provides a first glance at the variability of the SBH samples (Figure 3). Soybean processing facilities may provide SBH as loose particulates (SA-SE) or pelletized (SF-SH) to densify the biomass for transportation and further use elsewhere, such as in the preparation of feed for ruminants[40]. In addition to such differences in aggregation state, we also observe variations in color and presence of the contaminants (notably in SA-SC) coming from soybean agroindustrial processing.

Figure 3. Visualization of the soybean hull samples. Note the different colors, particle sizes, and aggregation states: (SA-SE) loose hulls and (SF-SH) pelletized hulls

Looking at SBH composition (Table 2), we note that insoluble carbohydrates make the main fraction (43-68 wt.%) of all samples. Among the insoluble carbohydrates, glucans are the main type, making 25-39 wt.% of the SBH composition. Other insoluble carbohydrates make minor yet significant contributions to the SBH composition: xylan (5-10 wt.%), arabinan (4-5 wt.%), galactan (2-4 wt.%), mannan (2-6 wt.%), and galacturonan (2-5 wt.%). Insoluble protein varies from 9-13 wt.%, while lignin (2-5 wt.%) and ash (4-6 wt.%) contents vary in a relatively narrow range. Contents of extractives also present notable variability: 2-4 wt.% for extractives in n-hexane and 15-27 wt.% for extractives in water and ethanol.

Table 2. Composition of soybean hulls given as wt.% of dry matter.

	Soybean hull samples							
Components	**SA**	**SB**	**SC**	**SD**	**SE**	**SF**	**SG**	**SH**
Ash	5.7 ± 0.1	5.4 ± 0.2	5.9 ± 0.0	4.5 ± 0.1	4.6 ± 0.0	4.7 ± 0.0	4.5 ± 0.1	4.4 ± 0.1
n-Hexane extractives	3.3 ± 0.2	4.4 ± 0.3	3.9 ± 0.2	3.2 ± 0.1	1.8 ± 0.2	3.4 ± 0.2	2.1 ± 0.2	1.6 ± 0.2
Water-ethanol extractives	25.7 ± 0.5	26.9 ± 0.5	25.2 ± 0.4	15.6 ± 0.6	16.1 ± 0.5	17.6 ± 0.2	15.5 ± 0.3	14.5 ± 0.3
In*. protein	11.4 ± 0.2	13.3 ± 0.1	12.4 ± 0.1	10.1 ± 0.1	10.0 ± 0.1	9.6 ± 0.1	9.1 ± 0.1	9.4 ± 0.0
In. lignin	2.5 ± 0.1	2.1 ± 0.2	4.6 ± 1.8	2.2 ± 0.1	2.3 ± 0.4	2.7 ± 0.4	4.8 ± 1.9	2.2 ± 0.1
In. carbohydrates	50.7 ± 1.0	46.4 ± 0.3	42.7 ± 4.6	60.7 ± 1.5	60.5 ± 1.3	59.9 ± 0.9	55.3 ± 2.8	67.5 ± 2.2
In. glucan	31.0 ± 0.3	29.1 ± 0.1	25.4 ± 2.4	35.2 ± 0.2	36.1 ± 0.1	34.4 ± 0.4	31.9 ± 0.5	38.5 ± 0.2
In. xylan	6.7 ± 0.2	6.3 ± 0.0	5.1 ± 0.8	9.1 ± 0.1	8.6 ± 0.2	8.3 ± 0.1	8.0 ± 0.4	10.5 ± 0.4
In. arabinan	4.1 ± 0.1	3.6 ± 0.1	3.6 ± 0.2	5.0 ± 0.4	4.9 ± 0.2	4.9 ± 0.1	4.2 ± 0.6	5.0 ± 0.2
In. Galactan	2.6 ± 0.1	2.3 ± 0.0	2.3 ± 0.1	3.1 ± 0.2	3.0 ± 0.2	3.5 ± 0.0	3.4 ± 0.1	3.5 ± 0.5
In. Mannan	3.5 ± 0.1	2.3 ± 0.1	4.2 ± 0.7	4.8 ± 0.3	4.1 ± 0.5	4.2 ± 0.1	5.2 ± 0.7	5.9 ± 0.7
In. galacturonan	2.8 ± 0.2	2.7 ± 0.0	2.1 ± 0.4	3.6 ± 0.3	3.8 ± 0.1	4.6 ± 0.2	2.6 ± 0.5	4.1 ± 0.2
Mass closure	99.3	98.5	94.8	96.3	95.2	98.0	91.4	99.5

*In. - insoluble

We evaluated the composition variability among SBH samples by Principal Component Analysis (PCA). The loadings plot (Figure 4b) shows remarkable relations between the SBH compositional attributes. PC1, accounting for 74 % of the variance, clearly group the insoluble carbohydrates (positive PC1 loading) with opposing variations (negative correlations) to the group of attributes including protein, extractives, and ash contents (negative PC1 loadings). In the scores plot (Figure 4a), SBH samples SA-SC appear at the quadrants of negative PC1, whereas samples SD-SH are at the quadrants of positive PC1. Noteworthy, this SBH grouping is unrelated to pelletizing (SF-SH in Figure 3). Rather, samples SA-SC present particles with variations in size and color (Figure 3) attributable to SBH contaminants such as soybean pods and other plant fractions. Moreover, the higher contents of extractives, protein, and ash in SA-SC additionally suggest relatively inefficient separation of the soybean components. These arguments

indicate the agroindustrial process (rather than the biological variability) is the dominant source of composition variability in the analyzed SBH sample set.

As we move our analysis to PC2, accounting for 16 % of the variance, we note that lignin contents are strongly represented in the loadings of this component (Figure 4b). Nevertheless, variations of lignin content (2-5 wt.%) may in some cases have comparable magnitudes to uncertainty in measurements, such as the ±2 % uncertainty in lignin contents of SC and SG samples (Table 2) that present high scores in PC2 (Figure 4a). Therefore, the significance of these variations must be judged with care. Carbohydrates such as galacturonan and mannan also contribute to PC2 with projections on PC2 axis either aligned (mannan, Man) or opposed (galacturonan, GalA) to lignin. As noted for PC1, pelletization (SF-SH) is also unrelated to the variations represented in PC2 (Figure 4a). With consideration of these results, it seems PC2 reflects, at least to some extent, biological variations in the contents of lignin and the proportions of the different carbohydrates present in SBH.

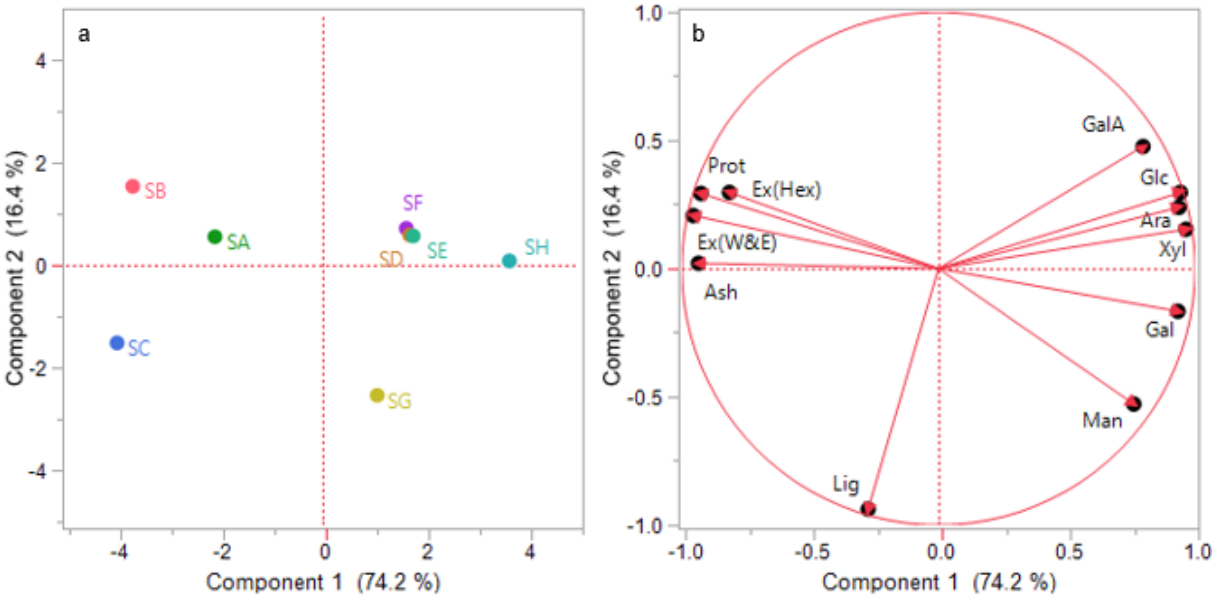

Figure 4. Principal component analysis of the soybean hull composition matrix. (a) Scores discriminating samples (SA-SH). (b) Loadings discriminating the relations between compositional attributes. GalA – Insoluble galacturonan, Glc -Insoluble glucan, Ara – Insoluble arabinan, Xyl – Insoluble xylan, Gal – Insoluble galactan, Man – Insoluble mannan, Lig – Insoluble Lignin, Ex(W&E) – Water-Ethanol extractives, Ex(Hex) – n-Hexane extractives, Prot – Insoluble Protein

Comparison with previous work allows us to further contextualize the SBH composition and variations presented in Table 2 and Figure 4. Previous studies of SBH reported cellulose as the most important cell-wall polysaccharide and estimated this component to range from 36-39 wt.% of SBH dry mass[9,21,41]. This is in fair agreement with our observation of 32-38 wt.% glucan in SD-SH, but our results demonstrate that this content is reduced to 25-31 wt.% in

SBH with higher contents of extractives, protein, and ash, such as those found in samples SA-SC (Table 2).

We also note in our results representative amounts of hemicelluloses and pectin, reported as xylan, arabinan, galactan, mannan, and galacturonan, varying from 17-29 wt.% of SBH mass. This range is in accordance with previous studies that reported total amounts of hemicelluloses and pectins ranging from 16-27 wt.%[9,21]. Hemicelluloses and pectin monosaccharides are representative of SBH structure as building blocks of a series of polysaccharides[42] located in primary and secondary plant cell-walls, which can potentially be used for SBH valorization.

The insoluble protein content is an important fraction in SBH composition, representing 10-14 wt.% of the biomass according to the previous studies[9,21]. Therefore, the observed range of 9.1-13.3 wt.% in our samples is within the variation reported in the literature. We also demonstrate a higher protein content (11.4-13.3 wt.%) in SA-SC which also have higher extractive and ash contents. SBH contains significantly higher amounts of protein compared to agricultural residues such as corn stover (4-9 wt.% protein) or wheat straw (2-6 wt.% protein), even though a similar range of cellulose contents (30-40 wt.%) is observed among these materials[21,43]. Here we highlight the high protein content as a key target for SBH valorization. Biochemical processing routes may generate fractions enriched in protein, increasing SBH value, as previously reported[21].

Contrary to carbohydrates and proteins, lignin content represents a minor fraction in SBH. A similar variation observed in our results (2.1-4.8 wt.%) has been reported[44,21], identifying lignin content to range from 2.4-5.8 wt.% depending on the seed variety analyzed. This is in line with the biological origins of lignin variability suggested by our PCA results (Figure 4). Lignin content in SBH is remarkably lower compared to other agroindustrial residues such as oat hulls (22-23 wt.% lignin)[20] or structural lignocelluloses such as sugarcane bagasse (23-24 wt.%)[45,46], hardwoods (15-30 wt.%) and softwoods (25-35 wt.%)[47]. Noteworthy, lignin makes a major contribution to biomass resistance to biological deconstruction (recalcitrance), and, therefore, the low lignin content is an opportunity for the valorization of SBH without the need for overcoming the lignin barriers.

We summarize the findings of this section by recalling that SBHs can be provided in either loose or pelletized states (Figure 3). We measured the contents of extractives, ashes, insoluble carbohydrates, and protein in SBH and our quantification is in fair agreement with previous studies. Moreover, we identified those remnants of pods and other extraneous matter (Figure 3) make the main source of composition variability in SBHs (PC1 in Figure 4), while

variability in lignin contents is minor, statistically independent (PC2 in Figure 4), and likely originated from biological variations.

4.3.2. Tisse-scale structure

A typical soybean seed (Figure 5a) contains specialized areas such as the hilum – a scar formed upon seed detachment from the pod structure, and the extrahilar region, which make the main mass fraction of the tissues represented in SBH[8]. We observed SBH fragments under the SEM and commonly identified three main layers (Figure 5b) from outside to inside: the palisade layer (PL), the hourglass layer (HL), and the parenchyma tissue (PA). These layers are characteristic structures of the extrahilar region of the hull[8]. Yellow arrows in Figure 5b reveal depressions in the outermost layer of the hull. These depressions in the palisade cuticle were observed in permeable soybean seeds and were related to the initial sites of hydration. They are observed not only in damaged hulls but also in intact seeds[8], evidencing the biological origin of these external depressions.

We have further investigated SBH tissue-scale structure by μCT, which allows non-invasive observation of the internal features of the biomass with micrometric resolution. A 3D reconstruction (Figure 5c) of a SBH fragment reveals the same layers (PL, HL, and PA) observed in SEM. However, the internal structure is also revealed by μCT, here shown as three orthogonal digital sections (Figure 5d-f) intersecting a common point of the tomogram. The yellow arrows in Figure 5d-f reveal cracks throughout the SBH cell layers that, similarly to depressions in the palisade cuticle, may be related to the hydration pathways of the material. The tissue cracks pointed at the tomogram, however, are better consistent with mechanical disruptions due to soybean agroindustrial processing.

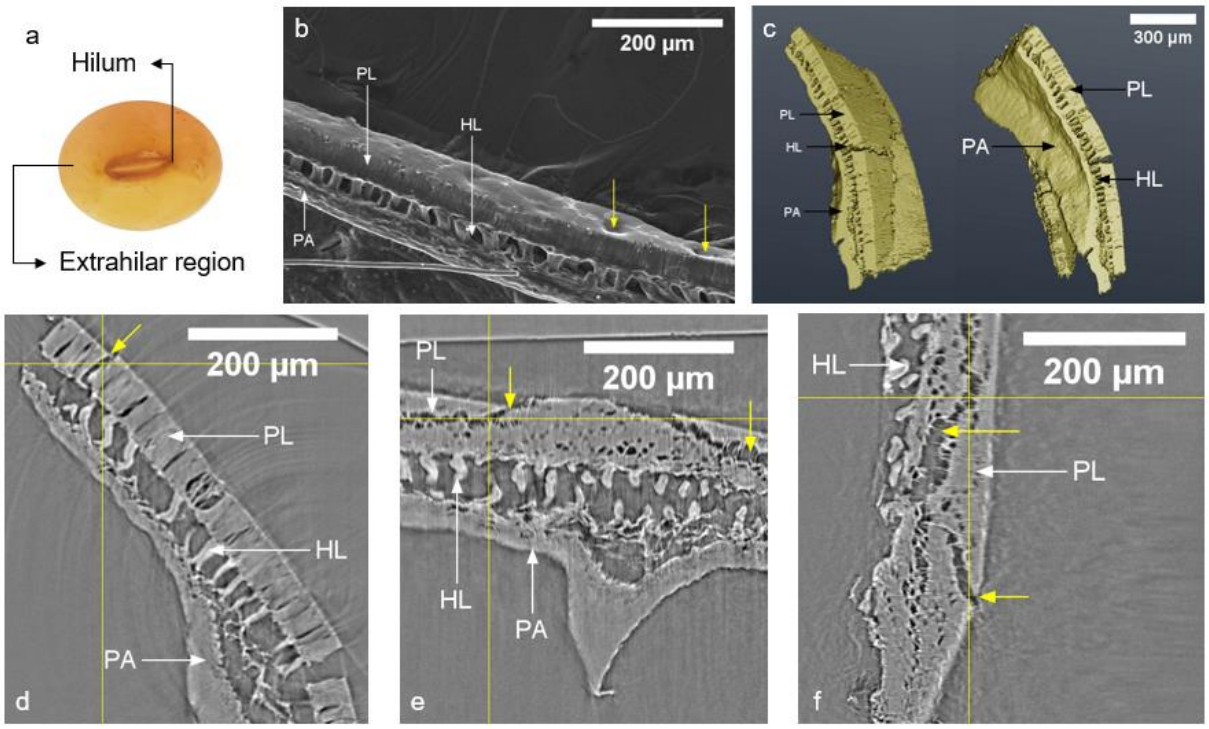

Figure 5. Visualization of soybean hull structures at the tissue scale. a – Hilum and extrahilar region: two main specialized structures in soybean seed; b – SEM image of a selected cross-section in which yellow arrows show depressions in the outermost layer of SBH; c – Three-dimensional rendered reconstruction of an SBH fragment imaged by µCT; d,e,f – orthogonal visualizations from µCT, in which yellow arrows show cracks in the internal structure of SBH. The orthogonal visualizations were obtained from the same point indicated at intersections of the yellow lines. Major extrahilar hull tissues are indicated. PL – palisade layers, HL – hourglass layer; PA – parenchyma

In further consideration of the SBH structure, we employed µRaman capabilities to investigate the SBH tissues. Polarized Raman spectra obtained for palisade cells (Figure 6a) revealed bands consistent with vibration modes of crystalline cellulose I [48,49]. More specifically, the observed Raman spectra from SBH palisade cells (Figure 6a) closely resemble the spectra from ramie fibers[49], which have been studied for a long time as a model system of cellulose from higher plants due to its natural cellulose purity and microfibrillar alignment. This comparison indicates that cellulose in the SBH palisade cells also presents significant purity and well-aligned microfibrils.

Considering the multitude of cellulose Raman bands, one highlights those bands that more strongly respond to changing laser polarization. The antisymmetric stretching of glycosidic linkages at 1095 cm^{-1} is much stronger upon vertical polarization (Figure 6a). On the other hand, bands such as the glycosidic symmetric stretching at 516 cm^{-1} are apparent only under horizontal polarization (Figure 6a). These responses to polarization are identical to those observed in ramie fibers, demonstrating the cellulose microfibrils in the palisade layer are well aligned to the vertical direction (i.e., perpendicular to SBH external surface). These essential Raman spectral features were unaltered as we moved the laser spot across different regions of the palisade cells.

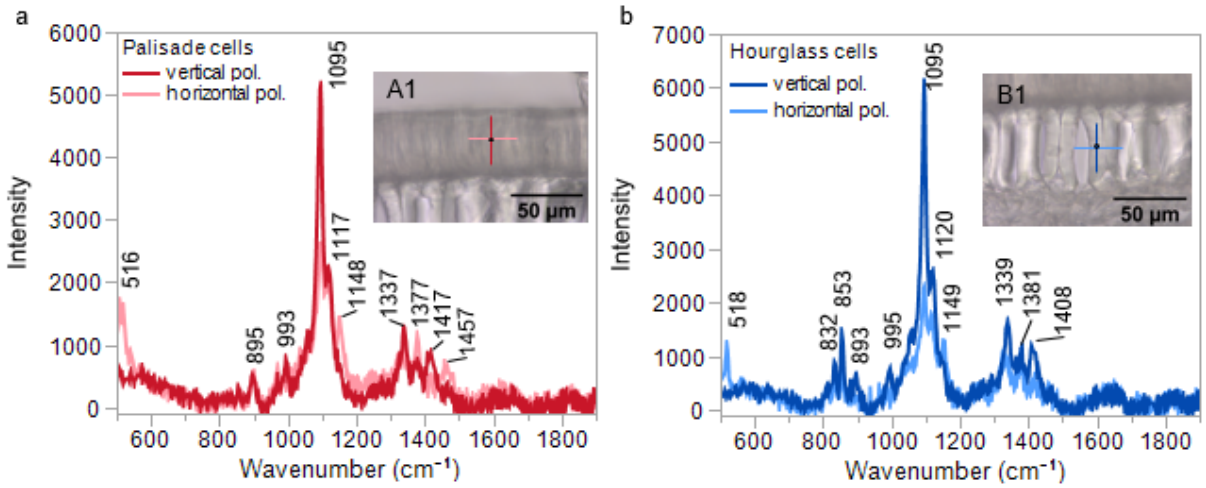

Figure 6. Polarized Raman spectra from (a) palisade cells and (b) hourglass cells using vertical and horizontal laser polarization. Location and polarization of the laser are indicated in the inset images

As we move to the hourglass cells (Figure 6b), we observe similar Raman signatures compared to the palisade cells of the SBH, including the signatures of crystalline cellulose I and vertical fibrillar alignment. However, the hourglass Raman spectra revealed two characteristic Raman bands at 832 and 853 cm^{-1} which are absent from palisade cells. Antisymmetric stretching of the α-glycosidic linkage in acidic pectins has been assigned to the 853 cm^{-1} band[50,51], which has also been reported not to overlap with other cell wall polymers and to be used as a marker band for pectin in plants[48]. In addition, the Raman band at 832 cm^{-1} has not been assigned to carbohydrates in previous studies but referred to bending of CH-ring groups and CH_2 rocking on hydrophobic amino acid tyrosine[52], which forms a characteristic doublet with a band at 856 cm^{-1}. Alongside other amino acids, tyrosine has been identified in SBH[21,53]. However, the assignment of these bands (832 and 853 cm^{-1}) to protein and more specifically to tyrosine is uncertain, although it is a possibility that deserves further investigation because it would help localize the protein content in SBH.

We also employed μRaman to investigate the tracheid bar, a characteristic structure in the SBH hilum region (Figure 5a)[8]. The Raman spectra of the tracheid bar (Figure 7) revealed remarkable differences compared to the palisade and hourglass layers (Figure 6).

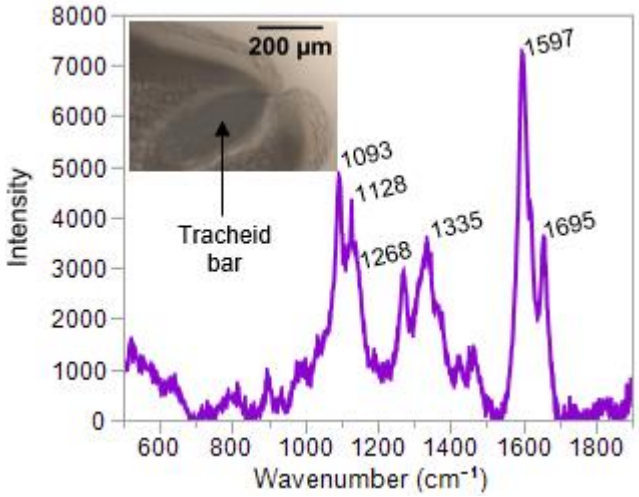

Figure 7. Raman spectra from soybean hull tracheid bar

Most notably, the tracheid bar presents Raman bands at 1268, 1597, and 1695 cm^{-1} that can be assigned to lignin[48,54,55]. This was the only region of SBH where we could find consistent Raman signals from lignin, evidencing the 2-5 wt.% lignin content (Table 2) is significantly localized in the SBH tracheid bar[55]. Therefore, the other regions of SBH have lignin contents much lower than the mean values observed in the composition analysis (Table 2). Moreover, the localized nature of lignin helps explain the variability of this component (represented mostly in PC2, Figure 4) found to be statistically independent of variations in carbohydrates and extractives (represented in PC1 of Figure 4).

4.3.3. Cellulose crystallites

XRD revealed characteristics of crystalline cellulose in SBH. The experimental area detector patterns are well represented by the CRAFS model (Figure 8a-b), which assumes the cellulose Iβ crystal structure[56], models the preferential orientation of the cellulose crystallites, and determines unit cell parameter and crystallite size from the fit to the experimental pattern[37]. As previously observed, the CRAFS model presents a characteristic misfit to the experimental pattern near 2θ ~30°, indicating the presence of stacking faults (mixed Iα-Iβ stacking) that are ubiquitous in cellulose I from higher plants[57].

The XRD analysis revealed that the cellulose crystallites of SBH are, on average, wider than the commonly found in lignocellulosic biomass. The wider crystallites are mainly noticed by the sharper (200) diffraction peak of SBH. In Figure 8d, we compare diffraction patterns from SBH and sugarcane bagasse, which has been intensely investigated using the same XRD

experimental and modeling tools[46]. The (200) peak of SBH is sharper, revealing the onset of the shoulder at lower 2θ assigned to (012) and (102) reflections, which are not apparent in the broader peaks from sugarcane bagasse. Translated into the mean crystallite width $L_{(200)}$, CRAFS analysis shows SBH $L_{(200)}$ = 3.5 nm, significantly greater than sugarcane bagasse, with $L_{(200)}$ = 2.9 nm[38,46] (Figure 8c).

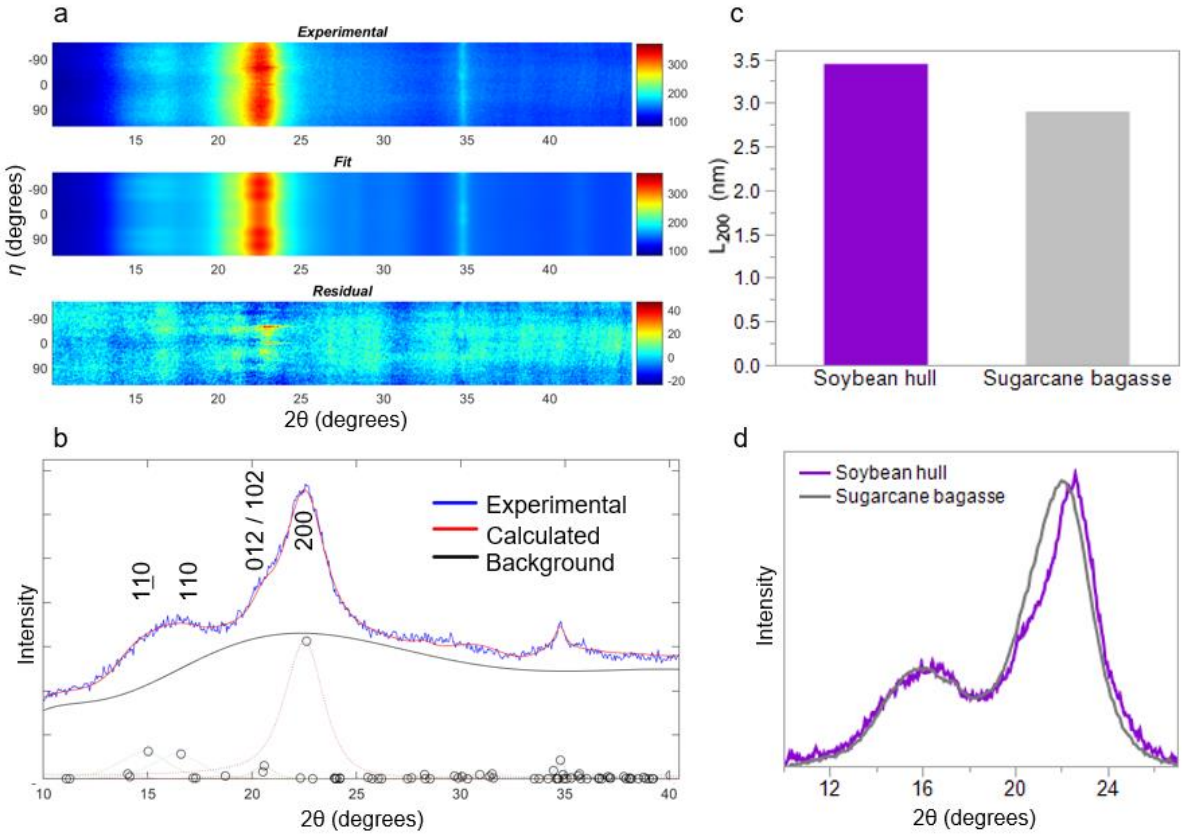

Figure 8. X-ray diffraction from SBH and comparison with parameters obtained from sugarcane bagasse. (a) SBH experimental, calculated, and residual (experimental–calculated) two-dimensional diffraction patterns are presented at the top, middle, and bottom, respectively. (b) Example of SBH diffractogram (η=0°). Experimental (blue line) and calculated (red line) intensities presented with contributions from the background (black line) and individual diffraction peaks (dotted gray lines). Circles identify positions from all cellulose Iβ diffraction peaks. (c) Crystal width L200 determined from SBH compared to sugarcane bagasse. (d) Comparison of diffractograms obtained from SBH and sugarcane bagasse.

Such wider crystallites in cellulose from higher plants have been previously reported in several species and tissues. For instance, wider cellulose crystallites are found in the gelatinous layer of tension wood, in bast fibers like flax, and most notably in cotton[58,59]. Wider crystallites are thought as indirect evidence for the presence of relatively pure and well-aligned cellulose. Cellulose microfibril alignment without spacers like hemicelluloses and pectins is thought to allow adjacent microfibrils to coalesce (co-crystallize), resulting in the observed gains in mean crystallite width. Based on μRaman evidence (Figure 6), these purity and orientation characteristics are present in both palisade and hourglass cells of SBH, but mainly in palisade cells

where the Raman spectra are consistent with quite pure cellulose (Figure 6). Therefore, besides the significant content of cellulose in SBH (Table 2), it is worth recognizing that significant regions of the biomass, most notably the palisade cells, have cellulose purity that seems sufficient to cause microfibril co-crystallization. We speculate this finding is also important for enzyme action on SBH, where simple cellulase preparations with minimum auxiliary activities (for pectins and hemicelluloses) may be sufficient for action on such regions of SBH with relatively pure cellulose.

4.3.4. Hydration

An important characteristic of biological materials is their interaction with water. As previously mentioned, plant biomass has a hierarchical multiscale structure[24,25] that generate multiscale interactions with water. From a practical perspective, water influences several aspects such as handling, storage, stability, and manufacturing of bio-based products[60]. Here we employed two thermal analysis techniques — dynamic vapor sorption (DVS) and calorimetric thermoporometry (CTP) — that probe complementary dimensions of biomass interactions with water[39].

DVS is primarily sensitive to the first molecular hydration layers contacting the solid matrix[39]. In Figure 9 (left) we show SBH moisture sorption isotherms and include, for comparison purposes, sorption isotherms from selected sugarcane tissues analyzed under identical conditions. The sorption isotherms have a typical sigmoidal behavior from type II isotherms according to the Brunauer classification[61]. Moreover, SBH pelleting did not impact water interactions probed by DVS, which is demonstrated by the similar isotherms observed for SBH in loose or pelletized forms. We also note that sorption isotherms from lignocelluloses shown here as comparison materials — sugarcane in two contrasting tissues and stages of development (young parenchyma and mature rind) — are similar to SBH. We further highlight that the observed SBH type II isotherms are also found in many other lignocelluloses and food materials[62,63], such as whole soybeans[64] or cereals (barley, rye, oat, and corn)[65]. These results and comparisons evidence that the moisture sorption in SBH is qualitatively indistinguishable from what is observed in a wide range of biological materials.

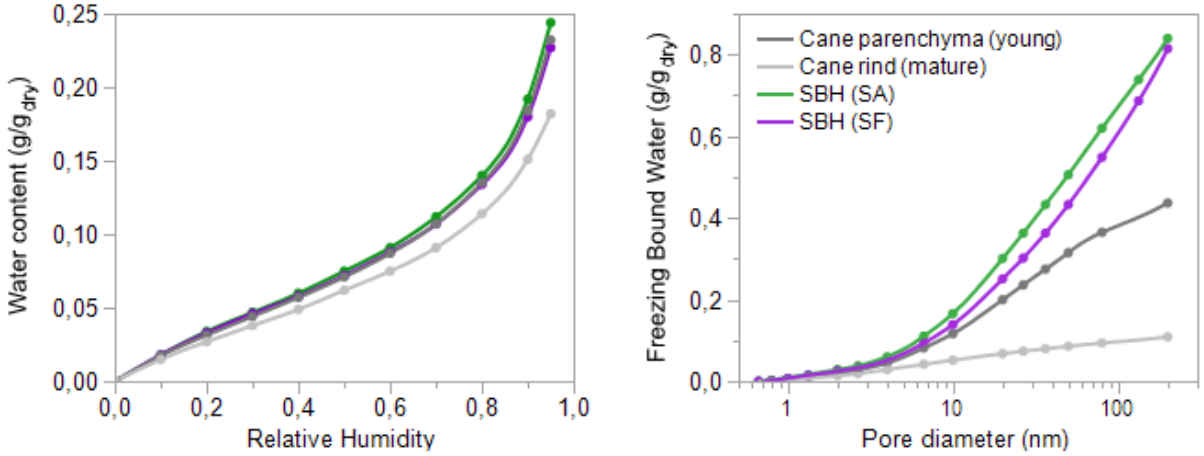

Figure 9. Vapor sorption isotherm (left) and thermoporometry profiles (right) of selected SBH samples. Sugarcane samples are included as a comparative lignocellulosic biomass with higher lignin contents.

Complementing the interactions probed by DVS, CTP probes water in nanometric pores of the materials saturated with water[39]. We first note that the CTP profiles for loose (SA) and pelletized (SF) SBH (Figure 9-right) are almost coincident, which indicates that nanoscale porosity is not significantly altered by the pelletizing process. Compared with the sugarcane tissues shown for reference, SBH are substantially more porous (*e.g.*, FBW profiles reach a maximum of 0.83 g/g at 200 nm pore diameter). We note that the porosity of mature sugarcane rind (FBW maximum 0.11 g/g) is similar to other highly lignified structural lignocelluloses such as softwoods and hardwoods (FBW maximum of 0.07 g/g and 0.06 g/g, respectively)[66]. On the other hand, the sugarcane young parenchyma (FBW maximum 0.44 g/g) is an example of tissue that does not play a mechanical role in the plant and is not yet mature and fully lignified, thus serving as a reference for higher porosity[63] but still presenting much lower nanoscale porosity than SBH. These results are in general agreement with lignin being a nanoscale pore filler, occupying voids in the cellulosic network from cell walls[67,68]. Indeed, the CTP profile from SBH resembles the CTP profiles observed in chemically delignified lignocelluloses[66], indicating that the low lignin contents (Table 2) and lignin localization in the tracheid bar of the hilum region (Figure 7) leave a highly porous polysaccharide network in the abundant extrahilar tissues of SBH.

4.3.5. Enzymatic hydrolysis

The enzymatic hydrolysis with commercial enzyme cocktails rich in cellulases, xylanases, β-glucanases, and pectinases demonstrated the high enzymatic digestibility of SBH. The amount of solubilized SBH was measured gravimetrically and increased from 15.5±0.5 wt.% (control) to

69.0±0.8 wt.% (enzyme treatment) (Figure 10). Sugars such as glucose and xylose were undetected in control experiments. In contrast, after enzyme treatments, sugars were detected and yields (referenced to stoichiometric potential) were high, reaching 80.7±1.0 wt.% for glucose and 86.8±1.3 wt.% for xylose (Figure 10). This result demonstrates the potential for enzymatic depolymerization of carbohydrates at high yields without any prior pretreatment applied to SBH.

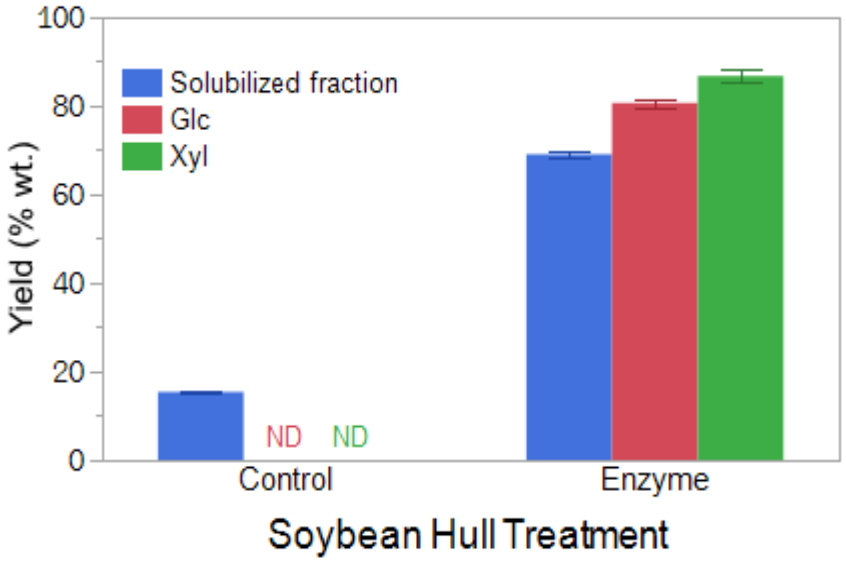

Figure 10. Yield (wt.%) of solubilized fraction, glucose (Glc), and xylose (Xyl) after submitting soybean hulls to enzymatic hydrolysis.

Noteworthy, although the low recalcitrance of SBH to biotechnological processing has been previously recognized, the magnitude of this effect for enzymatic hydrolysis of SBH using a comprehensive selection of enzyme activities was not yet clearly delineated. Mielenz et al (2011) previously reported 84.9 % of cellulose conversion of autoclaved SBH, measured by the residual glucose in the reaction media obtained after 13 days of enzymatic saccharification followed by fermentation[21]. Other studies reported pretreatment strategies to increase sugar yields due to relatively modest conversions for untreated SBH. Yoo et al (2011)[10] reported 40.8 % conversion of cellulose to glucose for untreated SBH, while Rojas et al (2014) reported a significantly lower conversion of 4 % after 24h hydrolysis using untreated SBH[69]. Moreover, Islam et al. (2017) reported conversion of approximately 30 % for untreated SBH using enzyme broths from *Trichoderma reesei* and *Aspergillus niger*[70]. We summarize these comparisons by noting that our result (Figure 10) is in line with the findings of Mielenz et al (2011), showing that high (>80 %) sugar yields can be obtained without applying any costly, energy-intensive pretreatment before enzymatic digestion of SBH.

4.4. Conclusions

Concluding, SBH have been previously observed to have inherent lower recalcitrance to enzymatic deconstruction as compared to other agricultural residues[10,12,21,69,70]. In this work, high carbohydrate yields (>80 %) in enzymatic hydrolysis (Figure 10) confirmed the potential for SBH biotechnological valorization without the need for biomass pretreatment. The high nanoscale porosity of SBH (Figure 9, right) especially for pore sizes greater than enzyme sizes ~5 nm[71] is understood as critical for greater enzymatic accessibility to the substrate, contributing to its lower recalcitrance. As previously mentioned, this higher accessibility is also related to the low, localized contents of lignin (Table 2 and Figure 7), reducing the nanoscale lignin barriers. Furthermore, the relative purity of cellulose in SBH hourglass and palisade layers evidenced directly by μRaman (Figure 6) and indirectly by wider cellulose crystals detected by XRD (Figure 8) also contribute to the relative low recalcitrance of SBH compared to other lignocellulosic feedstocks. These results provide a structural basis for understanding the low recalcitrance of SBH, paving the way for novel developments in SBH biotechnological valorization.

References

(1) Preece, K. E.; Hooshyar, N.; Zuidam, N. J. Whole Soybean Protein Extraction Processes: A Review. *Innovative Food Science & Emerging Technologies* **2017**, *43*, 163–172. https://doi.org/10.1016/j.ifset.2017.07.024.

(2) USDA. *World Agricultural Supply and Demand Estimates*; WASDE-599; 2020.

(3) FAO. *FAOSTAT Statistical Database*; Crop statistics; FAO, 2020.

(4) Liu, H.-M.; Li, H.-Y. Application and Conversion of Soybean Hulls. In *Soybean - The Basis of Yield, Biomass and Productivity*; Kasai, M., Ed.; InTech, 2017. https://doi.org/10.5772/66744.

(5) Porfiri, M. C.; Wagner, J. R. Extraction and Characterization of Soy Hull Polysaccharide-Protein Fractions. Analysis of Aggregation and Surface Rheology. *Food Hydrocolloids* **2018**, *79*, 40–47. https://doi.org/10.1016/j.foodhyd.2017.11.050.

(6) Bewley, J. D.; Black, M. *Seeds: Physiology of Development and Germination*; Springer US: Boston, MA, 1994. https://doi.org/10.1007/978-1-4899-1002-8.

(7) Souza, F. H. D. D.; Marcos-Filho, J. The Seed Coat as a Modulator of Seed-Environment Relationships in Fabaceae. *Rev. bras. Bot.* **2001**, *24* (4), 365–375. https://doi.org/10.1590/S0100-84042001000400002.

(8) Ma, F. Cracks in the Palisade Cuticle of Soybean Seed Coats Correlate with Their Permeability to Water. *Annals of Botany* **2004**, *94* (2), 213–228. https://doi.org/10.1093/aob/mch133.

(9) Corredor, D. Y.; Sun, X. S.; Salazar, J. M.; Hohn, K. L.; Wang, D. Enzymatic Hydrolysis of Soybean Hulls Using Dilute Acid and Modified Steam-Explosion Pretreatments. *J Biobased Mat Bioenergy* **2008**, *2* (1), 43–50. https://doi.org/10.1166/jbmb.2008.201.

(10) Yoo, J.; Alavi, S.; Vadlani, P.; Amanor-Boadu, V. Thermo-Mechanical Extrusion Pretreatment for Conversion of Soybean Hulls to Fermentable Sugars. *Bioresource Technology* **2011**, *102* (16), 7583–7590. https://doi.org/10.1016/j.biortech.2011.04.092.

(11) Sessa, D. J. Processing of Soybean Hulls to Enhance the Distribution and Extraction of Value-Added Proteins. *J. Sci. Food Agric.* **2004**, *84* (1), 75–82. https://doi.org/10.1002/jsfa.1612.
(12) Qing, Q.; Guo, Q.; Zhou, L.; Gao, X.; Lu, X.; Zhang, Y. Comparison of Alkaline and Acid Pretreatments for Enzymatic Hydrolysis of Soybean Hull and Soybean Straw to Produce Fermentable Sugars. *Industrial Crops and Products* **2017**, *109*, 391–397. https://doi.org/10.1016/j.indcrop.2017.08.051.
(13) Ferrer, A.; Salas, C.; Rojas, O. J. Dewatering of MNFC Containing Microfibrils and Microparticles from Soybean Hulls: Mechanical and Transport Properties of Hybrid Films. *Cellulose* **2015**, *22* (6), 3919–3928. https://doi.org/10.1007/s10570-015-0768-y.
(14) Sinclair, A.; Jiang, L.; Bajwa, D.; Bajwa, S.; Tangpong, S.; Wang, X. Cellulose Nanofibers Produced from Various Agricultural Residues and Their Reinforcement Effects in Polymer Nanocomposites: Research Article. *J. Appl. Polym. Sci.* **2018**, *135* (21), 46304. https://doi.org/10.1002/app.46304.
(15) Debiagi, F.; Faria-Tischer, P. C. S.; Mali, S. Nanofibrillated Cellulose Obtained from Soybean Hull Using Simple and Eco-Friendly Processes Based on Reactive Extrusion. *Cellulose* **2020**, *27* (4), 1975–1988. https://doi.org/10.1007/s10570-019-02893-0.
(16) Quosai, P.; Anstey, A.; Mohanty, A. K.; Misra, M. Characterization of Biocarbon Generated by High- and Low-Temperature Pyrolysis of Soy Hulls and Coffee Chaff: For Polymer Composite Applications. *R. Soc. open sci.* **2018**, *5* (8), 171970. https://doi.org/10.1098/rsos.171970.
(17) Herde, Z. D.; Dharmasena, R.; Sumanasekera, G.; Tumuluru, J. S.; Satyavolu, J. Impact of Hydrolysis on Surface Area and Energy Storage Applications of Activated Carbons Produced from Corn Fiber and Soy Hulls. *Carbon Resources Conversion* **2020**, *3*, 19–28. https://doi.org/10.1016/j.crcon.2019.12.002.
(18) Wang, S.; Shao, G.; Yang, J.; Liu, J.; Wang, J.; Zhao, H.; Yang, L.; Liu, H.; Zhu, D.; Li, Y.; Jiang, L. The Production of Gel Beads of Soybean Hull Polysaccharides Loaded with Soy Isoflavone and Their PH-Dependent Release. *Food Chemistry* **2020**, *313*, 126095. https://doi.org/10.1016/j.foodchem.2019.126095.
(19) Zhang, Y. J.; Liu, Q.; Zhang, W. M.; Zhang, Z. J.; Wang, W. L.; Zhuang, S. Gastrointestinal Microbial Diversity and Short-Chain Fatty Acid Production in Pigs Fed Different Fibrous Diets with or without Cell Wall-Degrading Enzyme Supplementation. *Livestock Science* **2018**, *207*, 105–116. https://doi.org/10.1016/j.livsci.2017.11.017.
(20) Cortivo, P. R. D.; Hickert, L. R.; Hector, R.; Ayub, M. A. Z. Fermentation of Oat and Soybean Hull Hydrolysates into Ethanol and Xylitol by Recombinant Industrial Strains of Saccharomyces Cerevisiae under Diverse Oxygen Environments. *Industrial Crops and Products* **2018**, *113*, 10–18. https://doi.org/10.1016/j.indcrop.2018.01.010.
(21) Mielenz, J. R.; Bardsley, J. S.; Wyman, C. E. Fermentation of Soybean Hulls to Ethanol While Preserving Protein Value. *Bioresource Technology* **2009**, *100* (14), 3532–3539. https://doi.org/10.1016/j.biortech.2009.02.044.
(22) Camiscia, P.; Giordano, E. D. V.; Brassesco, M. E.; Fuciños, P.; Pastrana, L.; Cerqueira, M. F.; Picó, G. A.; Woitovich Valetti, N. Comparison of Soybean Hull Pre-Treatments to Obtain Cellulose and Chemical Derivatives: Physical Chemistry Characterization. *Carbohydrate Polymers* **2018**, *198*, 601–610. https://doi.org/10.1016/j.carbpol.2018.06.125.
(23) Amaro Bittencourt, G.; Porto de Souza Vandenberghe, L.; Valladares-Diestra, K.; Wedderhoff Herrmann, L.; Fátima Murawski de Mello, A.; Sarmiento Vásquez, Z.; Grace Karp, S.; Ricardo Soccol, C. Soybean Hulls as Carbohydrate Feedstock for Medium to High-Value Biomolecule Production in Biorefineries: A Review. *Bioresource Technology* **2021**, *339*, 125594. https://doi.org/10.1016/j.biortech.2021.125594.
(24) Fratzl, P.; Weinkamer, R. Nature's Hierarchical Materials. *Progress in Materials Science* **2007**, *52* (8), 1263–1334. https://doi.org/10.1016/j.pmatsci.2007.06.001.

(25) Gibson, L. J. The Hierarchical Structure and Mechanics of Plant Materials. *J. R. Soc. Interface* **2012**, *9* (76), 2749–2766. https://doi.org/10.1098/rsif.2012.0341.
(26) Templeton, D. W.; Sluiter, A. D.; Hayward, T. K.; Hames, B. R.; Thomas, S. R. Assessing Corn Stover Composition and Sources of Variability via NIRS. *Cellulose* **2009**, *16* (4), 621–639. https://doi.org/10.1007/s10570-009-9325-x.
(27) Williams, C. L.; Westover, T. L.; Emerson, R. M.; Tumuluru, J. S.; Li, C. Sources of Biomass Feedstock Variability and the Potential Impact on Biofuels Production. *Bioenerg. Res.* **2016**, *9* (1), 1–14. https://doi.org/10.1007/s12155-015-9694-y.
(28) Negrão, D. R.; Ling, L. Y.; Bordonal, R. O.; Driemeier, C. Microscale Analyses of Mineral Particles in Sugar Cane Bagasse and Straw Shed Light on How Debris Can Be Incorporated into Biomass. *Energy Fuels* **2019**, *33* (10), 9965–9973. https://doi.org/10.1021/acs.energyfuels.9b02651.
(29) B. Hames; R. Ruiz; C. Scarlata; A. Sluiter; J. Sluiter; D. Templeton. *Preparation of Samples for Compositional Analysis*; Laboratory Analytical Procedure (LAP); Technical Report NREL/TP-510-42620; National Renewable Energy Laboratory: Golden, Colorado, 2008.
(30) A. Sluiter; B. Hames; R. Ruiz; C. Scarlata; J. Sluiter; D. Templeton. *Determination of Ash in Biomass*; Laboratory Analytical Procedure (LAP); Technical Report NREL/TP-510-42622; National Renewable Energy Laboratory: Golden, Colorado, 2008.
(31) Technical, A. Crude Protein--Combustion Method. In *AACC International Approved Methods*; AACC International, 2009. https://doi.org/10.1094/AACCIntMethod-46-30.01.
(32) A. Sluiter; R. Ruiz; C. Scarlata; J. Sluiter; D. Templeton. *Determination of Extractives in Biomass*; Laboratory Analytical Procedure (LAP); Technical Report NREL/TP-510-42625; National Renewable Energy Laboratory: Golden, Colorado, 2008.
(33) A. Sluiter; B. Hames; R. Ruiz; C. Scarlata; J. Sluiter; D. Templeton; D. Crocker. *Determination of Structural Carbohydrates and Lignin in Biomass*; Laboratory Analytical Procedure (LAP); Technical Report NREL/TP-510-42618; National Renewable Energy Laboratory: Golden, Colorado, 2012.
(34) Rasband, W. S. ImageJ, 1997.
(35) Marques, J. P. R.; Hoy, J. W.; Appezzato-da-Glória, B.; Viveros, A. F. G.; Vieira, M. L. C.; Baisakh, N. Sugarcane Cell Wall-Associated Defense Responses to Infection by Sporisorium Scitamineum. *Front. Plant Sci.* **2018**, *9*, 698. https://doi.org/10.3389/fpls.2018.00698.
(36) Ensikat, H. J.; Ditsche-Kuru, P.; Barthlott, W. Scanning Electron Microscopy of Plant Surfaces: Simple but Sophisticated Methods for Preparation and Examination. *Microscopy: Science, Technology, Applications and Education* **2010**, 248–255.
(37) Oliveira, R. P.; Driemeier, C. CRAFS: A Model to Analyze Two-Dimensional X-Ray Diffraction Patterns of Plant Cellulose. *J Appl Crystallogr* **2013**, *46* (4), 1196–1210. https://doi.org/10.1107/S0021889813014805.
(38) Driemeier, C.; Mendes, F. M.; Santucci, B. S.; Pimenta, M. T. B. Cellulose Co-Crystallization and Related Phenomena Occurring in Hydrothermal Treatment of Sugarcane Bagasse. *Cellulose* **2015**, *22* (4), 2183–2195. https://doi.org/10.1007/s10570-015-0638-7.
(39) Driemeier, C.; Mendes, F. M.; Oliveira, M. M. Dynamic Vapor Sorption and Thermoporometry to Probe Water in Celluloses. *Cellulose* **2012**, *19* (4), 1051–1063. https://doi.org/10.1007/s10570-012-9727-z.
(40) Blasi, D.; Drouillard, J.; Titgemeyer, E.; Paisley, S. *Soybean Hulls, Composition and Feeding Value for Beef and Dairy Cattle*; MF-2438; Kansas State University, 2000.
(41) Cassales, A.; de Souza-Cruz, P. B.; Rech, R.; Záchia Ayub, M. A. Optimization of Soybean Hull Acid Hydrolysis and Its Characterization as a Potential Substrate for Bioprocessing. *Biomass and Bioenergy* **2011**, *35* (11), 4675–4683. https://doi.org/10.1016/j.biombioe.2011.09.021.

(42) Carpita, N. C.; Gibeaut, D. M. Structural Models of Primary Cell Walls in Flowering Plants: Consistency of Molecular Structure with the Physical Properties of the Walls during Growth. *The Plant Journal* **1993**, *3* (1), 1–30. https://doi.org/10.1111/j.1365-313X.1993.tb00007.x.

(43) Aden, A.; Ruth, M.; Ibsen, K.; Jechura, J.; Neeves, K.; Sheehan, J.; Wallace, B.; Montague, L.; Slayton, A.; Lukas, J. *Lignocellulosic Biomass to Ethanol Process Design and Economics Utilizing Co-Current Dilute Acid Prehydrolysis and Enzymatic Hydrolysis for Corn Stover*; TP-510-32438; NREL - National Renewable Energy Laboratory, 2002; p 79.

(44) Mullin, W. J.; Xu, W. Study of Soybean Seed Coat Components and Their Relationship to Water Absorption. *J. Agric. Food Chem.* **2001**, *49* (11), 5331–5335. https://doi.org/10.1021/jf010303s.

(45) Laser, M.; Schulman, D.; Allen, S. G.; Lichwa, J.; Antal, M. J.; Lynd, L. R. A Comparison of Liquid Hot Water and Steam Pretreatments of Sugar Cane Bagasse for Bioconversion to Ethanol. *Bioresource Technology* **2002**, *81* (1), 33–44. https://doi.org/10.1016/S0960-8524(01)00103-1.

(46) Lima, C. S.; Rabelo, S. C.; Ciesielski, P. N.; Roberto, I. C.; Rocha, G. J. M.; Driemeier, C. Multiscale Alterations in Sugar Cane Bagasse and Straw Submitted to Alkaline Deacetylation. *ACS Sustainable Chem. Eng.* **2018**, *6* (3), 3796–3804. https://doi.org/10.1021/acssuschemeng.7b04158.

(47) Lourenço, A.; Pereira, H. Compositional Variability of Lignin in Biomass. In *Lignin - Trends and Applications*; Poletto, M., Ed.; InTech, 2018. https://doi.org/10.5772/intechopen.71208.

(48) Gierlinger, N.; Keplinger, T.; Harrington, M.; Schwanninger, M. Raman Imaging of Lignocellulosic Feedstock. In *Cellulose - Biomass Conversion*; Kadla, J., Ed.; InTech, 2013. https://doi.org/10.5772/50878.

(49) Wiley, J. H.; Atalla, R. H. Raman Spectra of Celluloses. In *The Structures of Cellulose*; Atalla, R. H., Ed.; ACS Symposium Series; American Chemical Society: Washington, DC, 1987; Vol. 340, pp 151–168. https://doi.org/10.1021/bk-1987-0340.ch008.

(50) Schulz, H.; Baranska, M. Identification and Quantification of Valuable Plant Substances by IR and Raman Spectroscopy. *Vibrational Spectroscopy* **2007**, *43* (1), 13–25. https://doi.org/10.1016/j.vibspec.2006.06.001.

(51) Gierlinger, N.; Sapei, L.; Paris, O. Insights into the Chemical Composition of Equisetum Hyemale by High Resolution Raman Imaging. *Planta* **2008**, *227* (5), 969–980. https://doi.org/10.1007/s00425-007-0671-3.

(52) Sjöberg, B.; Foley, S.; Cardey, B.; Enescu, M. An Experimental and Theoretical Study of the Amino Acid Side Chain Raman Bands in Proteins. *Spectrochimica Acta Part A: Molecular and Biomolecular Spectroscopy* **2014**, *128*, 300–311. https://doi.org/10.1016/j.saa.2014.02.080.

(53) Rackis, J. J.; Anderson, R. L.; Sasame, H. A.; Smith, A. K.; VanEtten, C. H. Soybean Amino Acids, Amino Acids in Soybean Hulls and Oil Meal Fractions. *J. Agric. Food Chem.* **1961**, *9* (5), 409–412. https://doi.org/10.1021/jf60117a021.

(54) Agarwal, U. P.; Ralph, S. A. FT-Raman Spectroscopy of Wood: Identifying Contributions of Lignin and Carbohydrate Polymers in the Spectrum of Black Spruce (Picea Mariana). *Appl Spectrosc* **1997**, *51* (11), 1648–1655. https://doi.org/10.1366/0003702971939316.

(55) Ji, Z.; Ma, J.-F.; Zhang, Z.-H.; Xu, F.; Sun, R.-C. Distribution of Lignin and Cellulose in Compression Wood Tracheids of Pinus Yunnanensis Determined by Fluorescence Microscopy and Confocal Raman Microscopy. *Industrial Crops and Products* **2013**, *47*, 212–217. https://doi.org/10.1016/j.indcrop.2013.03.006.

(56) Nishiyama, Y.; Langan, P.; Chanzy, H. Crystal Structure and Hydrogen-Bonding System in Cellulose Iβ from Synchrotron X-Ray and Neutron Fiber Diffraction. *J. Am. Chem. Soc.* **2002**, *124* (31), 9074–9082. https://doi.org/10.1021/ja0257319.

(57) Driemeier, C.; Francisco, L. H. X-Ray Diffraction from Faulted Cellulose I Constructed with Mixed Iα–Iβ Stacking. *Cellulose* **2014**, *21* (5), 3161–3169. https://doi.org/10.1007/s10570-014-0390-4.
(58) Leppänen, K.; Andersson, S.; Torkkeli, M.; Knaapila, M.; Kotelnikova, N.; Serimaa, R. Structure of Cellulose and Microcrystalline Cellulose from Various Wood Species, Cotton and Flax Studied by X-Ray Scattering. *Cellulose* **2009**, *16* (6), 999–1015. https://doi.org/10.1007/s10570-009-9298-9.
(59) Müller, M.; Burghammer, M.; Sugiyama, J. Direct Investigation of the Structural Properties of Tension Wood Cellulose Microfibrils Using Microbeam X-Ray Fibre Diffraction. *Holzforschung* **2006**, *60* (5), 474–479. https://doi.org/10.1515/HF.2006.078.
(60) Fontan, C. F.; Chirife, J.; Sancho, E.; Iglesias, H. A. Analysis of a Model for Water Sorption Phenomena in Foods. *J Food Science* **1982**, *47* (5), 1590–1594. https://doi.org/10.1111/j.1365-2621.1982.tb04989.x.
(61) Brunauer, S.; Deming, L. S.; Deming, W. E.; Teller, E. On a Theory of the van Der Waals Adsorption of Gases. *J. Am. Chem. Soc.* **1940**, *62* (7), 1723–1732. https://doi.org/10.1021/ja01864a025.
(62) A. Aviara, N. Moisture Sorption Isotherms and Isotherm Model Performance Evaluation for Food and Agricultural Products. In *Sorption in 2020s*; Kyzas, G., Lazaridis, N., Eds.; IntechOpen, 2020. https://doi.org/10.5772/intechopen.87996.
(63) Maziero, P.; Jong, J.; Mendes, F. M.; Gonçalves, A. R.; Eder, M.; Driemeier, C. Tissue-Specific Cell Wall Hydration in Sugarcane Stalks. *J. Agric. Food Chem.* **2013**, *61* (24), 5841–5847. https://doi.org/10.1021/jf401243c.
(64) Aviara, N. A.; Ajibola, O. O.; Oni, S. A. Sorption Equilibrium and Thermodynamic Characteristics of Soya Bean. *Biosystems Engineering* **2004**, *87* (2), 179–190. https://doi.org/10.1016/j.biosystemseng.2003.11.006.
(65) Ertugay, M. F.; Certel, M. Moisture Sorption Isotherms of Cereals at Different Temperatures. *Food / Nahrung* **2000**, *44* (2), 107–109. https://doi.org/10.1002/(SICI)1521-3803(20000301)44:2<107::AID-FOOD107>3.0.CO;2-F.
(66) Driemeier, C.; Oliveira, M. M.; Curvelo, A. A. S. Lignin Contributions to the Nanoscale Porosity of Raw and Treated Lignocelluloses as Observed by Calorimetric Thermoporometry. *Industrial Crops and Products* **2016**, *82*, 114–117. https://doi.org/10.1016/j.indcrop.2015.11.084.
(67) Ding, S.-Y.; Liu, Y.-S.; Zeng, Y.; Himmel, M. E.; Baker, J. O.; Bayer, E. A. How Does Plant Cell Wall Nanoscale Architecture Correlate with Enzymatic Digestibility? *Science* **2012**, *338* (6110), 1055–1060. https://doi.org/10.1126/science.1227491.
(68) Donaldson, L. A.; Wong, K. K. Y.; Mackie, K. L. Ultrastructure of Steam-Exploded Wood. *Wood Sci.Technol.* **1988**, *22* (2), 103–114. https://doi.org/10.1007/BF00355846.
(69) Rojas, M. J.; Siqueira, P. F.; Miranda, L. C.; Tardioli, P. W.; Giordano, R. L. C. Sequential Proteolysis and Cellulolytic Hydrolysis of Soybean Hulls for Oligopeptides and Ethanol Production. *Industrial Crops and Products* **2014**, *61*, 202–210. https://doi.org/10.1016/j.indcrop.2014.07.002.
(70) Islam, S. M. M.; Li, Q.; Loman, A. A.; Ju, L.-K. CO 2 -H 2 O Based Pretreatment and Enzyme Hydrolysis of Soybean Hulls. *Enzyme and Microbial Technology* **2017**, *106*, 18–27. https://doi.org/10.1016/j.enzmictec.2017.06.011.
(71) Payne, C. M.; Knott, B. C.; Mayes, H. B.; Hansson, H.; Himmel, M. E.; Sandgren, M.; Ståhlberg, J.; Beckham, G. T. Fungal Cellulases. *Chem. Rev.* **2015**, *115* (3), 1308–1448. https://doi.org/10.1021/cr500351c.

5. VARIABILITY OF SOUTH AMERICAN CORN DISTILLER'S DRIED GRAINS WITH SOLUBLES AND CONSEQUENCES FOR ENZYMATIC UPGRADING

Abstract

The corn ethanol industry generates vast amounts of distiller's dried grains with solubles (DDGS), a valuable coproduct source of carbohydrate and protein. The experience from traditional production regions, chiefly the United States, has shown that variability is a key factor for DDGS valorization. With the emergence of the corn ethanol industry in South America, the variability of DDGS in this new production region becomes a timely question. This work investigates DDGS samples supplied by facilities from Brazil, Paraguay, and Argentina, evidencing much higher variability than previously reported for other regions. Yeast content in DDGS is shown to be a minor factor, whereas the content of extractives and the proportion between corn fiber and protein are major ones. Enzymatic hydrolysis conducted with cocktails optimized for lignocellulose, corn fiber, and yeast fermentation shows complementarity and synergy acting on pre-extracted DDGS, and the response to enzymes can be correlated to the main compositional variations of DDGS. These results establish a basis for developing enzymatic strategies to upgrade DDGS with a rationalization of the main sources of substrate variability.

5.1. Introduction

Corn ethanol is currently the main platform for the production of biofuels in the world, delivering over 54 billion liters of renewable ethanol per year[1–3]. Ethanol is obtained from the fermentation of the high starch content (~70 wt.%) of corn kernels[4,5], while the main coproduct from the dry-grinding ethanol production process is the distiller's dried grains with solubles (DDGS)[6]. DDGS is composed mainly of the undigested fraction of grains[7], generating up to 80 kg DDGS for every 100 L of corn ethanol[8,9]. The United States promoted rapid growth of the corn ethanol industry in the first decade of the 2000s, becoming the biggest global producer of ethanol[10]. Brazil is the second global ethanol producer but uses sugarcane as the main feedstock[11]. Nevertheless, fast growth of the Brazilian corn ethanol industry is taking place in recent years, producing approximately 3.4 billion liters in 2021, an increase of ~330 % compared to 2018[2]. Neighboring South American countries, notably Argentina and Paraguay, are also participating in this wave of corn ethanol industrial deployment[12].

The abundance of DDGS motivates the development of applications for this coproduct as well as technological pathways to upgrade DDGS and enhance its value. Simultaneously with the rise of the corn ethanol industry in the United States, several studies indicated that a main point of concern was DDGS variability, which is caused by the type of grain, process design, operation practices, and other variations found among DDGS suppliers[5,6,8]. With the rise of corn

ethanol in South America, the variability of DDGS in this new production environment becomes a timely question. At least two characteristics of this new region contrast with those of the United States and should be highlighted. First, corn crops are adapted to the tropical and subtropical environments of South America, and this is expected to influence the DDGS variability originating from the type of grain[13]. Second, the industrial facilities in South America have been deployed later and adapted to local conditions, thus resulting in a different set of industrial technologies, which is expected to influence the process-related variability of DDGS[14].

DDGS is currently consumed mainly as an ingredient in animal feed production, chiefly for ruminant diets, given the high protein and caloric contents[15,16]. Variations in DDGS composition and quality bring uncertainties to the formulation of diets with possible negative impacts on animal production yields[5,17]. Despite the protein and energy values in DDGS, the polysaccharides (mainly cellulose and arabinoxylan) in the fiber fraction of DDGS are undigestible for monogastric livestock, such as poultry and swine, and need to be diminished to boost the use of DDGS in these important feed markets[18].

These limitations as a feed ingredient as well as the potential for obtaining additional value from DDGS have recently attracted substantial interest. A studied route for valorization is through the use of DDGS as a feedstock for microbial fermentation such as in the production of D-lactic acid, glycolipids, or alternative fuels such as butanol[17,19–21]. Another strategy to enhance the value of DDGS is through enzymatic pathways. Carbohydrate-active enzymes (*e.g.*, cellulases, xylanases, β-glucanases, and others) have been employed *in vitro* to increase both digestibility and fermentability of corn DDGS aiming at nutritional improvement for application in non-ruminant animal diets[22]. Similarly, cellulosic and hemicellulosic components of DDGS were targeted by a complex of enzymes containing endo- and exo-glucanases, hemicellulases, and β-glucosidase to obtain sugars fermentable by genetically modified yeast for further valorisation[23,24]. Additional enzyme classes such as phytases[25] and proteases[26] have also been employed aiming at enhancing the properties of hydrolyzed corn distillers solubles for applications as additives in food or feed industries. Nevertheless, the variability of DDGS remains a challenge for the valorization of this coproduct[27,28].

In this work, we bring into focus the compositional variability of corn DDGS obtained from production plants in South America. This is a timely contribution because the corn ethanol industry is expanding in this region and previous studies were devoted mainly to DDGS from North America and Europe[5,18,29–32]. In addition to compositional analysis and its statistics, this work generates samples of extracted DDGS and model substrates (de-starched corn and inactivated yeast) to dig into the origins of the observed DDGS variability. Moreover, enzymatic

essays are performed with enzyme cocktails targeting lignocellulosic biomass, corn fiber, and yeast fermentation to unveil the consequences of DDGS variability for enzymatic upgrading. The obtained results shed light on the specificities of South American DDGS and the importance of substrate variability for enzymatic upgrading.

5.2. Materials and Methods

5.2.1. Collection of the DDGS samples

Nine corn DDGS samples were kindly provided by five distinct ethanol production plants in Brazil, Argentina, and Paraguay. The facilities are located in two states of Brazil (Mato Grosso and Goiás), one province of Argentina (Córdoba), and two departments of Paraguay (Canindeyú and Caaguazú). All the DDGS samples were provided as commercialized by the facilities. They are commercially qualified by the suppliers as 'high-protein DDGS' (3 samples), 'high-fiber DDGS' (3 samples), or 'DDGS' without any additional qualifier (3 samples).

5.2.2. Preparation of extracted DDGS and model substrates

A subset of extracted DDGS was prepared by sequential extraction of selected samples of as-received DDGS to remove soluble solids from their composition. The first extraction step was conducted by sequential washings with n-hexane (10 % w/v) followed by filtration and drying at room temperature in a fume hood. The second extraction step was conducted by thoroughly washing with a mixture of distilled water and ethanol (10 % w/v) followed by filtration and drying overnight at 45 °C in a Heratherm oven (Thermo Fisher Scientific, Massachusetts, USA).

Two model substrates (de-starched corn and inactivated yeast) were prepared to emulate the main components of DDGS. De-starched corn was prepared from corn kernels procured from local suppliers and ground to pass through a 1 mm sieve using an A11 analytical mill (IKA, Germany). The ground material was submitted to enzymatic hydrolysis in 200 mL stainless-steel flasks, 30 % total solids contents at pH 5.0, 85 °C for 3 hours, using a commercial enzymatic product (Liquozyme®, Novozymes A/S, Denmark) with alpha-amylase activity and high efficiency in breaking down long starch chains in liquefaction step of corn ethanol production[33]. This enzymatic preparation was applied at 0.012 % (enzyme:corn weight), according to the supplier's recommendation. Sulfuric acid (72 %) was used for pH adjustment and a Labomat

incubator (Labomat BFA-12, Werner Mathis AG, Oberhasli, Switzerland) for continuous agitation and temperature control[34]. The remaining solid fraction was dried at 95 °C and submitted to the extraction procedure of the previous paragraph to conclude the preparation of the de-starched corn.

Inactivated yeast was prepared from a commercial dry yeast (*Saccharomyces cerevisiae*) provided by Novozymes A/S, Denmark. The dry yeast was hydrated with distilled water and 10 % (v/v) absolute ethanol was incorporated into the suspension to simulate end-of-fermentation conditions. The mixture was then incubated at boiling temperature to ensure yeast inactivation and removal of the ethanol content, a similar condition observed during the industrial distilling process. The remaining solid fraction was submitted to the previously described extraction procedure followed by freeze-drying and further oven-dried at 95 °C for 12h to conclude the preparation of the inactivated yeast.

5.2.3. Compositional analysis

Aliquots of the as-received DDGS, extracted DDGS, and model substrates were dried in a Heratherm oven (Thermo Fisher Scientific, Massachusetts, USA) at 45 °C for 3h and micronized with a knife-mill (MA048, Marconi, Brazil) using 1 mm output control screen[35]. Ash content was determined by calcination at 575 °C[36]. Protein content was determined with 200 mg aliquots by the Dumas combustion method for crude protein using a nitrogen analyzer (FP-628, Leco Corporation, St. Joseph, MI, USA)[37]. Conversion of nitrogen to protein used a mass conversion factor of 6.25 and ethylenediaminetetra-acetic acid (EDTA) as the nitrogen standard. Contents of extractives of as-received DDGS were determined by a two-steps analytical extraction in an automated system (Dionex Accelerated Solvent Extractor 350, Thermo Fisher Scientific, Massachusetts, USA) using n-hexane, followed by water and ethanol[38]. Oils and fats are expected as n-hexane extractives, while other non-structural components such as sugars, nitrogenous compounds, and waxes are expected as water-ethanol extractives.

Extracted samples were submitted to a two-step acid hydrolysis for the determination of structural carbohydrates and acid-insoluble residue (AIR). The filtrate was analyzed using high-performance liquid chromatography (HPLC). Monosaccharides (glucose, xylose, arabinose, galactose, and mannose) were quantified by HPLC (1200 Infinity, Agilent, Santa Clara, USA) with an Aminex HPX-87P column (300 mm x 7.8 mm) and a Microguard CarboP guard-column (Bio-Rad Laboratories, Hercules, USA). Polymeric sugar contents (glucan, xylan, arabinan, galactan, and mannan) were reported after correction for anhydrous stoichiometric fractions. AIR was

determined gravimetrically as the remaining residue after the two-step acid hydrolysis corrected for acid-insoluble ash[39]. Mass closure of as-received DDGS was calculated as the summation of n-hexane extractives, water-ethanol extractives, insoluble protein, AIR, polymeric sugars, and ashes. Mass closure of extracted DDGS and model substrates were calculated as the sum of insoluble protein, AIR, and polymeric sugars.

5.2.4. Enzymatic hydrolysis

Extracted DDGS and model substrates (2 g, dry weight) were submitted to enzymatic hydrolysis in 50 mL tubes, 10 % total solids contents, at pH 5.0, 50 °C for 72h. Sodium acetate buffer (100 mM) was used for pH control and an incubator (Fine PCR COMBI-D24) for temperature control and agitation. Commercial enzyme cocktails Cellic® Ctec3 HS, Frontia Fiber Wash®, and Vinotaste Pro®, obtained from Novozymes A/S, Denmark, were dosed based on dry substrate following the manufacturer's activity units (149.4 BHU-2-HS/g DDGS; 31.8 FXU-S/g DDGS; and 4.5 BGXU/g DDGS, respectively). These cocktails are hereafter aliased according to their typical target substrates: lignocellulose (LC), corn fiber (CF), and yeast fermentation (YF), respectively. Four types of enzymatic reactions were performed: with each cocktail used separately (LC, CF, or YF) and the three cocktails in combination using 1/3 of each enzymatic dose. After incubation, each sample was filtered and dried. The insoluble solids were weighed gravimetrically, while the solubilized fraction was obtained by subtraction. Supernatants were used for sugar determination by HPLC after enzymatic hydrolysis.

5.2.5. Statistical analysis

The experimental data matrices were analyzed using the statistical package from JMP 14 (SAS, EUA). Principal component analysis (PCA) was employed to evaluate three distinct types of datasets. First, the matrix of compositional data of as-received DDGS was analyzed to identify clustering between distinct attributes (chemical components) and distinct DDGS samples. Second, an analogous PCA procedure was employed to the extracted DDGS and model substrates so the variability of samples disregarding extractive contents could be investigated. Third, the matrix of enzymatic hydrolysis responses was analyzed by PCA to rationalize the impact of the different enzyme treatments on the set of extracted DDGS and model substrates. Finally, correlations between enzymatic responses and compositions of extracted samples were evaluated and plotted as a color-coded correlation matrix.

5.3. Results and Discussion

5.3.1. Variability of as-received DDGS

The variability of the nine corn DDGS samples (SA-SI) is first noticeable by visual inspection (Figure 11), which reveals variations in color and particle size. The commercial qualifiers of the products, 'high-protein DDGS' (SA, SE, SH), 'high-fiber DDGS' (SB, SF, SI), or simply 'DDGS' (SC, SD, SG), do not show any remarkable relation with the observed colors and particle sizes.

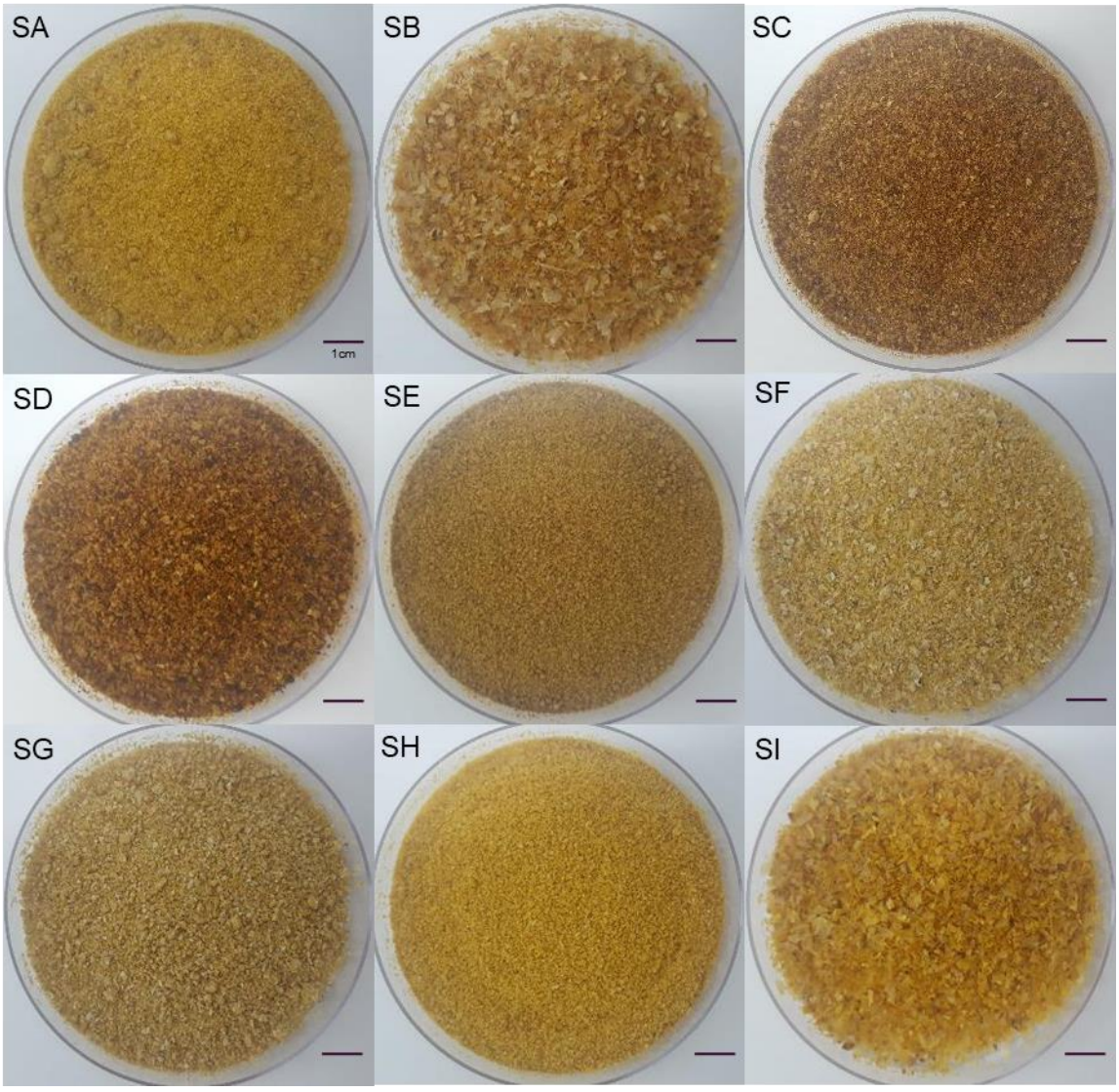

Figure 11. Visualization of the as-received corn DDGS samples (SA-SI). Note variations in color and particle size.

The chemical composition of the as-received DDGS (Table 3) shows remarkable variability across the investigated samples set. For example, wide ranges were observed for n-

hexane extractives (3.8-12.5 wt.%), water-ethanol extractives (7.3-36.9 wt.%), insoluble protein (11.2-47.4 wt.%), and total insoluble carbohydrates (10.0-39.9 wt.%). Large variations are also found within the carbohydrates: glucan (6.0-17.0 wt.%), xylan (1.6-12.7 wt.%), arabinan (1.5-7.7 wt.%), galactan (0-2.9 wt.%), and mannan (0-4.5 wt.%).

Table 3. Composition of as-received corn DDGS given as wt.% dry matter

	DDGS samples								
Component	SA	SB	SC	SD	SE	SF	SG	SH	SI
Ash	2.1±0.1	5.2±0.1	2.6±0.1	4.5±0.1	2.6±0.1	1.3±0.1	1.1±0.1	2.4±0.1	5.8±0.1
n-Hexane extractives	12.0±0.2	10.4±0.6	8.9±0.7	10.6±0.3	8.9±0.6	6.2±0.2	3.8±0.2	9.9±0.4	12.5±0.1
Water-ethanol extractives	18.6±0.1	36.9±0.3	21.6±0.1	32.8±0.2	17.1±0.2	7.3±0.9	7.3±2.9	15.2±1.1	36.8±1.2
In*. protein	39.0±0.1	12.7±0.1	26.2±0.2	19.6±0.1	47.4±0.1	31.1±0.2	32.7±0.2	43.9±0.1	11.2±0.1
AIR	11.4±1.9	6.2±0.8	4.6±0.4	6.1±0.6	3.7±0.3	7.5±0.3	7.4±0.4	6.6±1.1	3.7±0.2
In. carbohydrates	10.0±0.4	30.1±1.6	31.4±0.6	23.8±1.4	21.9±0.4	39.9±1.3	39.2±2.5	29.2±2.5	31.4±1.4
In. glucan	6.0±0.1	16.2±0.7	13.9±0.1	10.9±0.4	12.4±0.1	15.3±0.8	17.0±1.0	15.9±1.8	13.4±0.5
In. xylan	1.6±0.1	7.4±0.5	10.4±0.3	7.1±0.7	2.8±0.1	12.7±0.2	11.0±0.7	5.3±0.2	9.2±0.4
In. arabinan	1.5±0.1	4.4±0.3	5.2±0.1	4.4±0.2	2.2±0.1	7.7±0.1	6.9±0.4	4.4±0.1	5.2±0.2
In. galactan	ND	1.4±0.1	2.0±0.1	1.4±0.1	ND	2.9±0.1	2.5±0.3	0.9±0.1	2.2±0.2
In. mannan	0.9±0.1	0.7±0.1	ND	ND	4.5±0.1	1.4±0.1	1.8±0.1	2.7±0.3	1.4±0.1
Mass closure	93.1	101.6	95.3	97.4	101.5	93.4	91.4	107.2	101.3

*In. – insoluble, ND – not detected

Variability in the DDGS composition can be further appreciated with PCA applied to the data in Table 3. PC1×PC2 explains 78 % of the variance. The loadings plot (Figure 12B) shows three main groups of attributes. The first group is represented by the insoluble carbohydrates glucan, xylan, arabinan, and galactan. The second group of attributes is represented by ash, extractives in n-hexane, and extractives in water-ethanol. The third group of attributes is represented by insoluble protein, mannan, and AIR. The loadings (Figure 12B) of these three main groups of attributes are approximately distributed at the vertices of a triangle, which is characteristic of three independent factors of variation submitted to one constraint, in this case, the theoretical mass closure of 100 %.

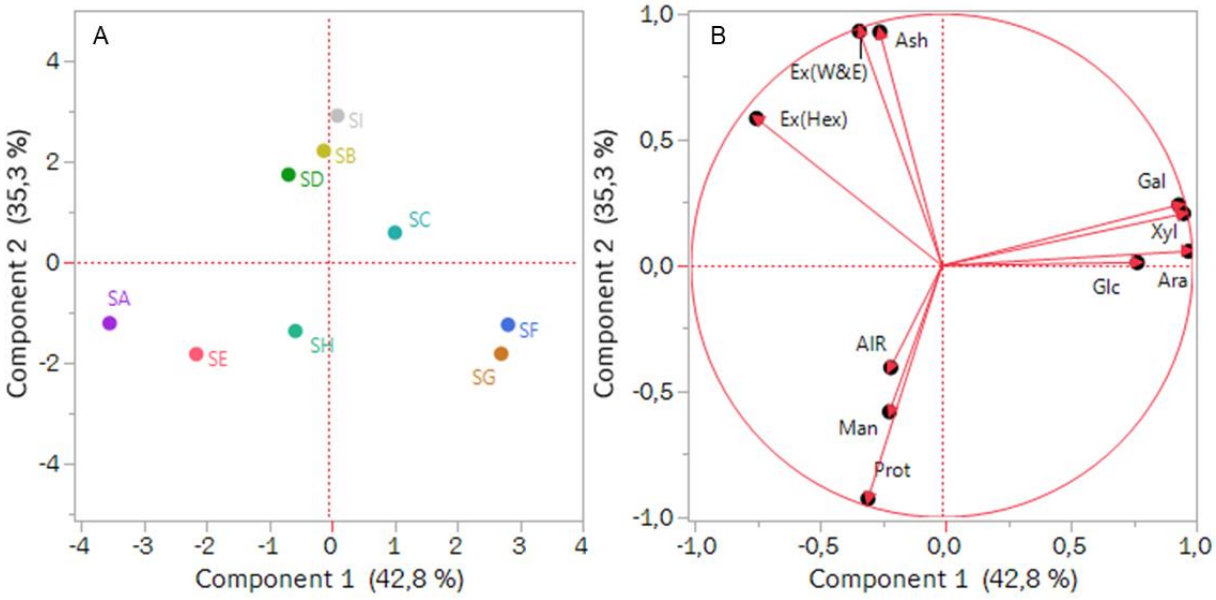

Figure 12. Principal component analysis of the as-received corn DDGS composition matrix. (A) Scores discriminating samples (SA-SH). (B) Loadings discriminating the relations between compositional attributes. Glc -Insoluble glucan, Ara – Insoluble arabinan, Xyl – Insoluble xylan, Gal – Insoluble galactan, Man – Insoluble mannan, AIR – Acid insoluble residue, Ex(W&E) – Water-Ethanol extractives, Ex(Hex) – n-Hexane extractives, Prot – Insoluble Protein.

The scores plot (Figure 12A) discriminates the corn DDGS samples according to their compositional profiles. Notably, the samples commercialized as high-protein DDGS (SA, SE, and SH) indeed show higher protein contents (39.0-47.4 wt.%) in Table 3 and appear clustered in the quadrant of negative PC1 and PC2 (Figure 12A), consistent with the protein loading in this quadrant (Figure 12B). The remaining DDGS samples are scattered in the other quadrants of the plot, and the group commercialized as high-fiber DDGS (SB, SF, SI) cannot be discriminated from the group of DDGS without a commercial qualifier (SC, SD, SG). These six DDGS samples have relatively low protein content with variability also spanning a wide interval (11.2-31.1 wt.%), while the other components also vary within wide ranges (Table 3).

The pronounced variability observed in the South American corn DDGS of the present study (Table 3 and Figure 12) is critical for the development of new technologies for upgrading this coproduct and deserves to be framed in comparison with previous studies. A recent study[40] on the nutritional potential of 8 samples of Brazilian corn distiller's grains also showed remarkable variability. For instance, in this previous study protein content of DDGS samples varied from 16.2 to 51.7 wt.%[40], similar to the range (11.2-47.4 wt.%) observed in the present work (Table 3). These variations in South American corn DDGS are much higher than the results found in previous variability studies conducted with corn DDGS. For instance, one study evaluated 72 samples of corn DDGS collected from 21 ethanol plants in the United States, observing protein content within 27.1-36.4 wt.%, with an average of 31.4 wt.%[29]. Another study[9]

that analyzed 4 samples of corn DDGS obtained from four different facilities in the United States also found a similar range of protein content (28.0-31.1 wt.%), while contents of carbohydrates glucan (18.3-20.1 wt.%), xylan (10.4-11.9 wt.%), and arabinan (5.5-6.2 wt.%) also varied in much narrower ranges compared with the observations of the present work (Table 3). These comparisons evidence that corn DDGS from South America has remarkably high variability, enhancing the concerns with variability as a critical factor for the valorization of this coproduct.

5.3.2. Detailing variability through the analysis of extracted DDGS and model substrates

Analysis of the samples of extracted DDGS allows the reduction of the variability of the sample set by experimentally diminishing the presence of one group of attributes (extractives) that behave as an independent component of variation (Figure 12B). In this section, four distinct DDGS samples are selected (SA, SC, SE, and SI) for further investigation because these samples are distributed in the observed range of variability of insoluble compounds. These samples of extracted DDGS (eSA, eSC, eSE, and eSI) together with the model substrates (de-starched corn and inactivated yeast) are here used to re-evaluate the variability of the DDGS set, this time without the contribution of extractives. The model substrates supposedly represent the isolated components of which extracted DDGS samples are composed, helping the understanding of the variations in DDGS. The composition of this set of extracted samples is presented in Table 4.

Table 4. Composition of the selected samples of extracted DDGS and model substrates given as wt.% dry matter.

Component	Extracted DDGS samples				Extracted model substrates	
	eSA	eSC	eSE	eSI	de-starched corn	inactivated yeast
In*. protein	55.4±0.1	37.0±0.5	61.2±0.1	21.5±0.2	37.6±0.5	42. 5±0.1
AIR	12.0±0.1	11.5±0.2	12.4±0.7	9.7±1.2	8.3±1.3	7.0±1.5
In. carbohydrates	34.1±0.8	47.2±1.1	26.5±1.5	60.6±0.5	48.7±1.6	49.7±0.5
In. glucan	16.9±0.2	17.5±0.3	14.3±0.6	22.9±0.1	23.1±0.5	30.6±0.1
In. xylan	6.5±0.2	14.5±0.4	3.7±0.2	20.6±0.1	12.6±0.6	ND
In. arabinan	5.3±0.2	8.9±0.2	2.4±0.2	12.1±0.1	8.2±0.3	2.3±0.2
In. galactan	1.9±0.1	3.4±0.1	0.8±0.2	3.5±0.1	2.9±0.1	2.1±0.1
In. mannan	3.6±0.1	2.8±0.1	5.2±0.3	1.5±0.1	2.0±0.1	14.3±0.1
Mass closure	101.6	95.7	100.1	91.8	94.5	98.7

*In. – insoluble ND- not detected

The composition of the de-starched corn in this work (Table 4) presents contents of glucans (23.1 wt.%), xylan (12.6 wt.%), arabinan (8.2 wt.%), and AIR (8.3 wt.%) in fair agreement with a previous study, which determined similar contents of glucans (25.1 wt.%), xylan (14.5 wt.%), arabinan (11.5 wt.%) and AIR (7.5 wt.%) using the same analytical method[34]. In de-starched corn, cellulose and arabinoxylans remain the main structural polysaccharides of the cell walls of the corn fiber. Other hemicelluloses such as glucomannan and arabinogalactan are present in lower amounts. Cellulose is the major polysaccharide in unwashed corn pericarp, which derives from the outer layers of corn kernels[41]. Arabinoxylans, formed from a linear backbone of β-1,4-xylopyranosyl residues substituted mainly with α-arabinofuranosyl residues, is a major polymer in the cell walls of grains such as corn[23,42]. Cellulose, arabinoxylans, and the minor hemicellulosic components become concentrated after de-starching to produce corn ethanol.

Cell walls from the yeast used in ethanol fermentation are an additional insoluble component of the DDGS, but the yeast contribution is not well known due to a lack of standardization in estimation methods[27,43]. Polysaccharides and glycoproteins are the major components of fungal cell walls, and the cell walls of the yeast *Saccharomyces cerevisiae* contain β-1,3-glucans, β-1,6-glucans, chitin, and mannoproteins[44,45]. Notably, previous studies demonstrated the presence of linkages between the different components of the yeast cell wall, such as between chitin and β-1,3-glucan, as well as between β-1,6-glucan, β-1,3-glucan, and the glycoproteins[46].

Comparison of the composition of the extracted DDGS, de-starched corn, and inactivated yeast in Table 4 evidence the lack of unambiguous compositional markers to contrast the two model substrates. Protein, AIR, glucan, arabinan, galactan, and mannan are present in both model substrates. On the other hand, xylan is absent from inactivated yeast, but xylan contents are highly variable among the extracted DDGS (3.7-20.6 wt.%), thus challenging the usefulness of xylan as a compositional marker. Mannan is also a case of interest because the content in the inactivated yeast (14.3 wt.%) is much higher than in the de-starched corn (2.0 wt.%), but also mannan content is highly variable among the extracted (1.5-5.2 wt.%) (Table 4) and the as-received DDGS (0-4.5 wt.%) (Table 3). Therefore, due to the lack of specific univariate markers, multivariate statistics are henceforth employed to check the underlying patterns in the composition of extracted DDGS and model substrates.

PCA of the compositional matrix of extracted DDGS and model substrates is presented in Figure 13, with PC1×PC2 explaining 96.2 % of the variance. The scores plot (Figure 13A) shows inactivated yeast well separated from the extracted DDGS samples (eSE, eSA, eSC, and eSI) and the de-starched corn. Moreover, the displacement of the inactivated yeast is

approximately orthogonal to the dispersion of extracted DDGS, indicating that yeast content is a minor factor in the DDGS variability.

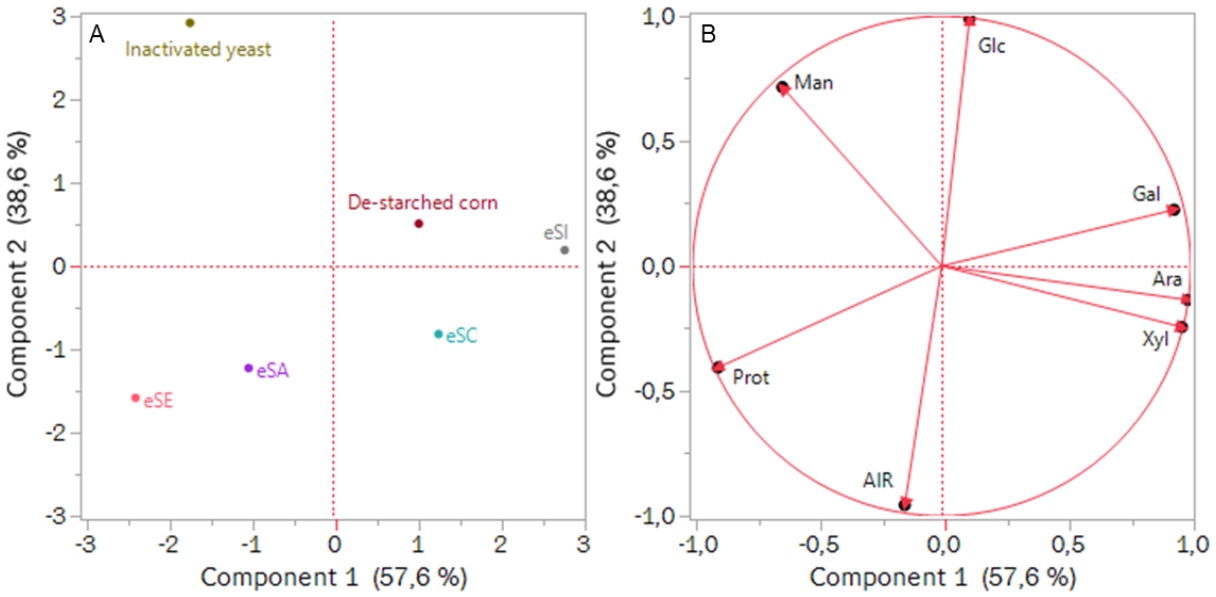

Figure 13. Principal component analysis of the composition matrix of the extracted DDGS and model substrates. (A) Scores discriminating samples (eSA, eSC, eSE, eSI, de-starched corn, and inactivated yeast). (B) Loadings discriminating the relations between compositional attributes. Glc -Insoluble glucan, Ara – Insoluble arabinan, Xyl – Insoluble xylan, Gal – Insoluble galactan, Man – Insoluble mannan, AIR – Acid insoluble residue, Prot – Insoluble Protein.

The loadings plot (Figure 13B) shows mannan in the same quadrant of inactivated yeast (Figure 13A), consistent with mannan content being an important (though unspecific) compositional marker of yeast. Moreover, the dispersion of extracted DDGS (Figure 13A) is along the direction between the loadings of protein and carbohydrates xylan, arabinan, and galactan (Figure 13B), indicating that the proportion between protein and corn fiber is the main differentiator among the extracted DDGS. Glucan and AIR, aligned respectively to positive and negative PC2 (Figure 13B) are relatively unspecific compositional markers to the presence of yeast in extracted DDGS, since PC2 lies in-between the dispersion of extracted DDGS and the displacement of the datapoint of the inactivated yeast (Figure 13A).

By establishing model substrates and re-evaluating a set of distinct extracted DDGS we further rationalized the main sources of variation in South American sourced DDGS, resulting from contributions of yeast, corn fiber, and protein. Previous studies determined that yeast may account for up to 20-50 % of the protein in DDGS[43,47]. However, in our sample set the presence of yeast represents a minor factor in DDGS variability, whereas the proportion of protein and corn fiber is a major source of variation. This finding likely results from the implementation of new technologies in the conventional dry-grind ethanol process, which includes fractionation

either before or after the fermentation step that results in the production of high-protein and high-fiber DDGS co-products[6,31]. The variability of the DDGS evaluated in this study (Table 3 and Table 4), in particular the proportion between corn fiber and protein, is therefore mainly attributed to the set of industrial technologies used in the South American facilities, which needs to be considered for the development of efficient upgrading strategies of DDGS.

5.3.3. Enzymatic hydrolysis

This study employed three different commercial enzymatic cocktails referred to as LC, CF, and YF (see methods section 5.3.4). None of these cocktails is tailored for DDGS upgrading. The LC cocktail is efficient for lignocellulose conversion into fermentable sugars, containing mainly cellulases and hemicellulases, besides AA9 oxidases and β-glucosidases[48]. The CF cocktail contains a mix of cellulases and xylanases to soften the corn fiber structure and ease the release of oil and starch[49]. The YF cocktail is a blend produced by fermentation of non-GM microorganisms that includes mainly pectinases and β -1,3-glucanases; it is dedicated to fermentation processes and has activity on yeast cell walls[50]. These three enzymatic cocktails provide profiles of enzymatic activities with a complementarity that is well suited to investigate the impacts of DDGS variability.

Enzymatic hydrolysis resulted in measurable solubilization of total mass, protein, glucose, xylose, arabinose, galactose, and mannose (Table 5). For all the tested samples of extracted DDGS and model substrates, the total mass solubilized by the enzymatic treatments (5.3-50.1 wt.% on total solids) is well above the control experiments (*i.e.*, without enzymes), demonstrating the effectiveness of the enzymatic treatments. Solubilization of protein (up to 5 wt.%) and monomeric glucose (up to 8 wt.%) in DDGS samples were markedly higher than monomeric xylose (up to 0.9 wt.%), arabinose (up to 1.2 wt.%), galactose (up to 0.3 wt.%), and mannose (up to 0.3 wt.%). These are low levels of xylose, arabinose, galactose, and mannose considering their contents in the extracted samples (Table 4). Such low solubilizations may result, at least in part, from the incomplete hydrolysis of the recalcitrant hemicelluloses of corn fiber[51–53]. Part of these hemicellulose fractions may be solubilized as oligomeric forms and contribute to the significant share of unaccounted components of solubilization (Table 5). This is a hypothesis that deserves further investigation in future studies.

Table 5. Results of enzymatic hydrolysis

Sample	Enzyme treatment	Solubilization (wt.% on total solids)							
		Total mass	Protein	Glucose†	Xylose†	Arabinose†	Galactose†	Mannose†	Unaccounted*
eSA	Control	1.24±0.13	0	0.09±0.01	0.01±0.01	0.01±0.01	0	0	1.13
	LC	14.62±0.23	1.76±0.21	4.43±0.02	0.60±0.01	0.95±0.01	0.12±0.01	0.14±0.01	6.63
	CF	11.17±0.28	0.63±0.22	2.87±0.01	0.41±0.01	0.59±0.04	0.05±0.01	0.09±0.01	6.53
	YF	10.98±0.10	2.37±0.46	5.31±0.06	0.05±0.01	0.39±0.01	0.09±0.01	0.09±0.01	2.68
	Combination	17.98±0.62	1.41±0.33	6.91±0.07	0.67±0.01	1.08±004	0.26±0.01	0.16±0.01	7.49
eSC	Control	1.63±0.12	1.58±0.10	0.01±0.01	0	0.03±0.01	0	0	0
	LC	18.37±0.28	3.28±0.26	6.84±0.07	0.88±0.02	0.87±0.02	0.14±0.01	0.30±0.01	6.07
	CF	12.73±0.10	1.93±0.18	3.57±0.02	0.52±0.01	0.52±0.01	0.05±0.01	0.13±0.01	6.01
	YF	8.98±0.10	2.42±0.06	4.32±0.01	0.07±0.01	0.53±0.01	0.15±0.01	0.07±0.01	1.40
	Combination	19.37±0.40	3.00±0.42	8.06±0.10	0.94±0.01	1.11±0.02	0.33±0.01	0.22±0.01	5.71
eSE	Control	1.59±0.04	0.97±0.08	0.02±0.01	0	0.01±0.01	0.07±0.01	0	0.51
	LC	14.11±0.19	3.46±0.25	3.93±0.02	0.58±0.01	0.81±0.01	0.08±0.01	0.11±0.01	5.15
	CF	10.51±0.32	1.57±0.27	2.68±0.03	0.40±0.01	0.57±0.01	0.06±0.01	0.08±0.01	5.16
	YF	15.88±0.05	5.04±0.12	6.17±0.01	0.07±0.01	0.51±0.01	0.12±0.01	0.10±0.01	3.87
	Combination	21.25±0.05	4.35±0.25	7.72±0.03	0.73±0.01	1.18±0.01	0.33±0.01	0.14±0.01	6.81
eSI	Control	4.44±0.30	1.19±0.37	1.11±0.01	0.06±0.01	0.03±0.01	0	0	2.05
	LC	15.70±0.30	3.23±0.41	7.30±0.05	0.55±0.01	0.65±0.01	0.10±0.01	0.16±0.01	3.72
	CF	11.64±0.23	1.91±0.04	3.76±0.03	0.36±0.02	0.35±0.01	0.04±0.01	0.03±0.04	5.12
	YF	9.21±0.01	3.07±0.29	5.64±0.09	0.04±0.05	0.38±0.01	0.09±0.01	0.03±0.01	(0.05)
	Combination	15.71±0.34	3.00±0.18	7.36±0.01	0.59±0.01	0.93±0.01	0.27±0.01	0.11±0.01	3.44
De-starched corn	Control	5.22±0.25	1.52±0.84	0.15±0.01	0	0.01±0.01	0.05±0.01	0.07±0.01	3.42
	LC	19.62±0.63	2.51±0.48	10.90±1.20	0.83±0.06	1.11±0.09	0.11±0.01	0.04±0.01	4.13
	CF	15.51±0.12	1.70±0.14	5.06±0.05	0.53±0.05	0.74±0.04	0.05±0.01	0.05±0.01	7.37
	YF	12.22±0.17	2.69±0.39	9.00±1.22	0.06±0.02	0	0.12±0.01	0.06±0.01	0.28
	Combination	20.26±0.50	2.42±0.21	10.71±0.09	0.83±0.01	1.36±0.02	0.34±0.01	0.04±0.01	4.57
Inactivated yeast	Control	2.11±0.12	1.28±0.11	0.01±0.01	0	0	0	0	0.73
	LC	9.01±0.17	4.85±0.08	3.65±0.01	0	0	0.04±0.01	0.07±0.01	0.40
	CF	5.33±0.22	3.01±0.13	2.02±0.01	0	0	0	0	0.22
	YF	50.12±0.07	17.58±0.09	20.49±0.01	0	0	0	0	12.07
	Combination	37.57±1.80	12.60±0.81	16.95±0.22	0	0	0.09±0.01	0.02±0.01	7.90

* Unaccounted: total solubilization minus the solubilization of protein, glucose, xylose, arabinose, galactose, and mannose. † Measured as free monomeric sugars.

The dataset in Table 5 was analyzed by PCA to investigate the multivariate patterns resulting from the enzymatic treatments (Figure 14). The effects of the different treatments (control, LC, CF, YF, and combination) prevail over the variability of the extracted DDGS, as observed by the dominant grouping by colors (representing enzyme treatments) rather than symbols (representing substrates). The treatment with the combination of cocktails produced the strongest effect, evidencing the synergy of the three complementary cocktails acting in concert.

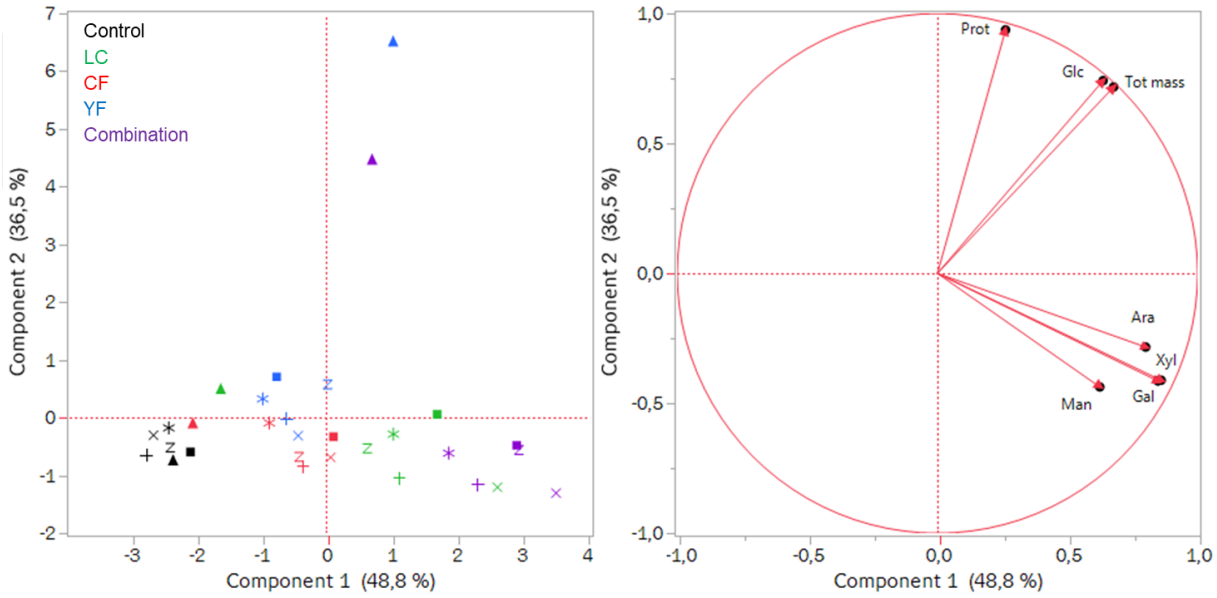

Figure 14. Principal component analysis of enzymatic hydrolysis responses from extracted DDGS and extracted model substrates. (A) Scores discriminating samples by symbols (eSA: +, eSC: x, eSE: z, eSI: *, de-starched corn: ■, inactivated yeast: ▲) and treatments by color (Control – black, LC: green, CF: red; YF: Blue, Combination: Purple). (B) Loadings discriminating the relations between analyzed responses. Tot Mass – Solubilized total mass (wt.%), Prot – Solubilized protein (wt.%), Glc - Solubilized glucose (wt.%), Ara – Solubilized arabinose (wt.%), Xyl – Solubilized xylose (wt.%), Gal – Solubilized galactose (wt.%), Man – Solubilized mannose (wt.%).

The inactivated yeast (▲ in Figure 14A) behaves as an outlier after processing with the YF cocktail, either alone (blue triangle) or in combination with the other cocktails (purple triangle). That is, response to the YF cocktail is a marker of the presence of yeast. Such a yeast marker is also unspecific, like the mannan content from compositional analysis (Table 4 and Figure 13). The YF cocktail solubilizes mainly glucose and protein from the yeast, as visible in the loadings plot (Figure 14A) and solubilization raw data (Table 5). The high solubilization of glucose and protein from yeast cells, mainly composed of bioactive β-glucans with β-(1→6) or β-(1→3) linkages and protein[46,54], is therefore in agreement with the main enzyme activities present in the YF cocktail.

The dataset of Table 5 was reanalyzed by PCA excluding the inactivated yeast, which provides a closer look into the DDGS and model de-starched corn without the yeast outlier

(Figure 15). The prevalence of different enzymatic treatments (control, LC, CF, YF, and combination) over the variability of DDGS is replicated in this new analysis, observed by the dominant grouping by colors (representing enzyme treatments) rather than symbols (representing substrates). Interestingly, the response to the YF cocktail (blue symbols in Figure 15A) still appears related to protein solubilization (Figure 15B). The datapoint of de-starched corn (■, blue square) is close to the extracted DDGS samples eSA, eSC, and eSI (blue symbols +, x, and *, respectively), suggesting these samples of DDGS have low yeast content. On the other hand, the eSE sample has a distinguishable response to the YF cocktail (blue z in Figure 15A). This result, in line with the higher mannan content (Table 4), suggests higher yeast content in eSE.

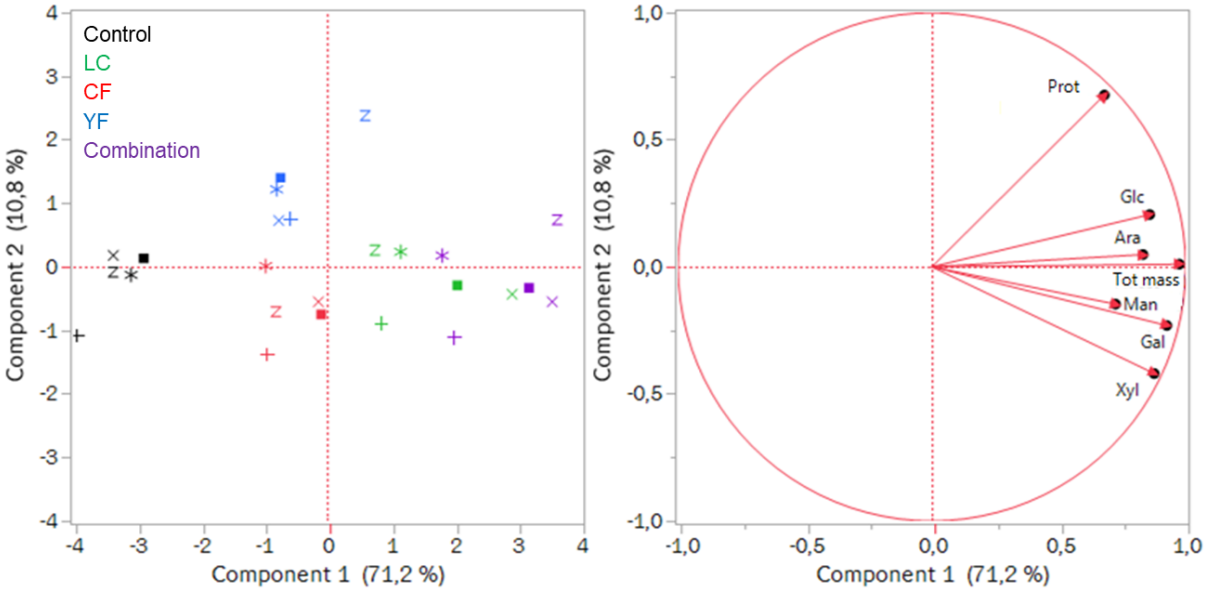

Figure 15. Principal component analysis of enzymatic hydrolysis responses from extracted DDGS and extracted de-starched corn. (A) Scores discriminating samples by symbols (eSA: +, eSC: x, eSE: z, eSI: *, de-starched corn: ■) and treatments by color (Control – black, LC: green, CF: red; YF: Blue, Combination: purple). (B) Loadings discriminating the relations between analyzed responses. Tot Mass – Solubilized mass (wt.%), Prot – Solubilized protein (wt.%), Glc -Solubilized glucose (wt.%), Ara – Solubilized arabinose (wt.%), Xyl – Solubilized xylose (wt.%), Gal – Solubilized galactose (wt.%), Man – Solubilized mannose (wt.%).

As previously stated, enzymatic hydrolysis resulted in high solubilization of total mass, protein, and monomeric glucose, in contrast with much lower solubilizations of monomeric xylose, arabinose, galactose, and mannose (Table 5). These stronger responses (solubilization of total mass, protein, and monomeric glucose) were chosen for analysis of correlations with the DDGS compositional attributes. The inactivated yeast was removed from the dataset used in this correlation analysis to avoid bias due to its outlying behavior. Moreover, the contents of AIR were also removed from the analysis because it is an unspecific compositional component (Table 4). The correlation matrix (Figure 16) highlights in blue and red, respectively, the positive and

negative correlations between the responses for each enzyme treatment and the chemical content in the extracted DDGS and the de-starched corn. The statistical significance of the correlations must be judged with care because only 5 data points (4 extracted DDGS and 1 de-starched corn) were used for the calculation of each correlation. Because of this limitation, rather than discussing individual correlations, we henceforth discuss Figure 16 based on sets of correlations with congruent behavior.

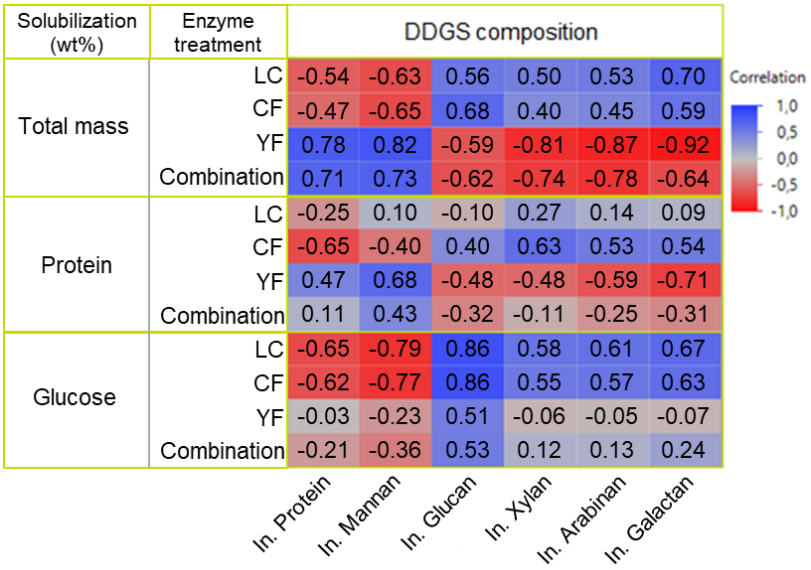

Figure 16. Correlation matrix between compositional components of extracted substrates (columns) and response to enzymatic treatments (rows).

Total solubilization in Figure 16 discriminates two sets of compositional attributes and two sets of enzyme cocktails. One set of attributes is made of insoluble carbohydrates (glucan, xylan, arabinan, and galactan), except for mannan, which is grouped with protein, as previously observed in the compositional data (Figure 12B). The contents of these carbohydrates are positively correlated with the solubilizations promoted by the LC and CF cocktails, whereas they are negatively correlated with the response promoted by the YF cocktail used alone or in combination. These results support that enzyme cocktails rich in cellulases and xylanases boost solubilization of DDGS with high fiber content, while the enzyme activities present in YF (*i.e.*, β-1,3-glucanase) enhance solubilization of the yeast fraction present in DDGS material.

Protein solubilization in Figure 16 shows a pattern like the one observed for total mass, although with weaker correlations. For the glucose solubilization shown in Figure 16, the main difference is the weaker correlations (*i.e.*, lower magnitudes) for the hydrolysis conducted with the YF cocktail alone or in combination. This result arises, at least in part, from the unspecific nature

of the glucan content, present in both the corn fiber and the inactivated yeast (Table 4 and Figure 13) and thus responding to all the tested enzymatic cocktails (Table 5).

The utilization of complementary enzymatic activities in this study was demonstrated to be beneficial for enhancing the solubilization of structural components of a set of highly variable DDGS samples. We observe higher total mass, protein, and monomeric glucose solubilization compared to the other components (monomeric xylose, arabinose, galactose, and mannose) typical of corn fiber structure. Arabinoxylan, the major component of cereal fiber, is highly complex and branched in corn affecting the accessibility to enzymatic degradation[16,23]. Previous studies reported low solubilization of corn fiber compared to other grains (*i.e.*, wheat and oat)[55] and highlighted that synergies between enzyme activities, such as xylanases, proteases, and pectinases enhance solubilization of DDGS components[16,56]. We demonstrate in this study that complementary enzyme activities that target main DDGS components should be employed with consideration of the highly variable DDGS produced in South America.

5.4. Conclusions

The availability of corn DDGS is growing rapidly in South America. In this work, DDGS samples obtained from corn ethanol facilities in Brazil, Argentina, and Paraguay were investigated. They presented higher compositional variability in comparison to previously reported data from other regions (*e.g.*, the United States). The compositional variations could be rationalized as resulting from three main factors: extractives, protein, and corn fiber contents. The presence of yeast in DDGS was demonstrated, but not quantified, and is indicated to be a minor component of the observed variability. Enzymatic hydrolysis with cocktails specialized in lignocellulose, corn fiber, and yeast revealed complementary and synergistic effects for the solubilization of DDGS structural components in a highly variable set of pre-extracted DDGS. Furthermore, the response to enzymes could be correlated to the main compositional variations of DDGS, establishing a basis for enzymatic strategies to upgrade DDGS with consideration of its patterns of variability.

References

(1) RFA, Renewable Fuels Association. *Annual World Fuel Ethanol Production*; 2022.
(2) CONAB, Companhia Nacional de Abastecimento. *Séries Históricas Das Safras - Cana-de-Açúcar - Indústria*; 2022.

(3) Lee, U.; Kwon, H.; Wu, M.; Wang, M. Retrospective Analysis of the U.S. Corn Ethanol Industry for 2005 – 2019 : Implications for Greenhouse Gas Emission Reductions. *Biofuels, Bioprod. Bioref.* **2021**, *15* (5), 1318–1331. https://doi.org/10.1002/bbb.2225.
(4) Mohammadi Shad, Z.; Venkitasamy, C.; Wen, Z. Corn Distillers Dried Grains with Solubles: Production, Properties, and Potential Uses. *Cereal Chem* **2021**, *98* (5), 999–1019. https://doi.org/10.1002/cche.10445.
(5) Belyea, R. L.; Rausch, K. D.; Clevenger, T. E.; Singh, V.; Johnston, D. B.; Tumbleson, M. E. Sources of Variation in Composition of DDGS. *Animal Feed Science and Technology* **2010**, *159* (3–4), 122–130. https://doi.org/10.1016/j.anifeedsci.2010.06.005.
(6) U.S. Grains Council. *DDGS User's Handbook - Precision DDGS Nutrition*, 4th ed.; 2018.
(7) Iram, A.; Cekmecelioglu, D.; Demirci, A. Distillers' Dried Grains with Solubles (DDGS) and Its Potential as Fermentation Feedstock. *Appl Microbiol Biotechnol* **2020**, *104* (14), 6115–6128. https://doi.org/10.1007/s00253-020-10682-0.
(8) Buenavista, R. M. E.; Siliveru, K.; Zheng, Y. Utilization of Distiller's Dried Grains with Solubles: A Review. *Journal of Agriculture and Food Research* **2021**, *5*, 100195. https://doi.org/10.1016/j.jafr.2021.100195.
(9) Kim, Y.; Hendrickson, R.; Mosier, N. S.; Ladisch, M. R.; Bals, B.; Balan, V.; Dale, B. E.; Dien, B. S.; Cotta, M. A. Effect of Compositional Variability of Distillers' Grains on Cellulosic Ethanol Production. *Bioresource Technology* **2010**, *101* (14), 5385–5393. https://doi.org/10.1016/j.biortech.2010.02.054.
(10) USDA, United States Department of Agriculture. *Distillers' Dried Grains with Solubles (DDGS) Production*; Agricultural Marketing Service.
(11) Chum, H. L.; Warner, E.; Seabra, J. E. A.; Macedo, I. C. A Comparison of Commercial Ethanol Production Systems from Brazilian Sugarcane and US Corn. *Biofuels, Bioprod. Bioref.* **2014**, *8* (2), 205–223. https://doi.org/10.1002/bbb.1448.
(12) Alonso Pippo, W.; Alves, A. Corn Ethanol in Brazil: Analyzing the Prospect of Becoming a Widespread Practice in South America. *Sugar Tech* **2022**, *24* (3), 857–869. https://doi.org/10.1007/s12355-021-01103-1.
(13) Eckert, C. T.; Frigo, E. P.; Albrecht, L. P.; Albrecht, A. J. P.; Christ, D.; Santos, W. G.; Berkembrock, E.; Egewarth, V. A. Maize Ethanol Production in Brazil: Characteristics and Perspectives. *Renewable and Sustainable Energy Reviews* **2018**, *82*, 3907–3912. https://doi.org/10.1016/j.rser.2017.10.082.
(14) Silva, A. L. da; Castañeda-Ayarza, J. A. Macro-Environment Analysis of the Corn Ethanol Fuel Development in Brazil. *Renewable and Sustainable Energy Reviews* **2021**, *135*, 110387. https://doi.org/10.1016/j.rser.2020.110387.
(15) Zhao, J.; Wang, D.; Li, Y. Proteins in Dried Distillers' Grains with Solubles: A Review of Animal Feed Value and Potential Non-food Uses. *J Am Oil Chem Soc* **2021**, *98* (10), 957–968. https://doi.org/10.1002/aocs.12516.
(16) Pedersen, M. B.; Dalsgaard, S.; Arent, S.; Lorentsen, R.; Knudsen, K. E. B.; Yu, S.; Lærke, H. N. Xylanase and Protease Increase Solubilization of Non-Starch Polysaccharides and Nutrient Release of Corn- and Wheat Distillers Dried Grains with Solubles. *Biochemical Engineering Journal* **2015**, *98*, 99–106. https://doi.org/10.1016/j.bej.2015.02.036.
(17) Chatzifragkou, A.; Kosik, O.; Prabhakumari, P. C.; Lovegrove, A.; Frazier, R. A.; Shewry, P. R.; Charalampopoulos, D. Biorefinery Strategies for Upgrading Distillers' Dried Grains with Solubles (DDGS). *Process Biochemistry* **2015**, *50* (12), 2194–2207. https://doi.org/10.1016/j.procbio.2015.09.005.
(18) Kim, Y.; Mosier, N. S.; Hendrickson, R.; Ezeji, T.; Blaschek, H.; Dien, B.; Cotta, M.; Dale, B.; Ladisch, M. R. Composition of Corn Dry-Grind Ethanol by-Products: DDGS, Wet Cake, and Thin Stillage. *Bioresource Technology* **2008**, *99* (12), 5165–5176. https://doi.org/10.1016/j.biortech.2007.09.028.

(19) Zaini, N. A. M.; Chatzifragkou, A.; Tverezovskiy, V.; Charalampopoulos, D. Purification and Polymerisation of Microbial D-Lactic Acid from DDGS Hydrolysates Fermentation. *Biochemical Engineering Journal* **2019**, *150*, 107265. https://doi.org/10.1016/j.bej.2019.107265.
(20) Sen, S.; Borah, S. N.; Sarma, H.; Bora, A.; Deka, S. Utilization of Distillers Dried Grains with Solubles as a Cheaper Substrate for Sophorolipid Production by Rhodotorula Babjevae YS3. *Journal of Environmental Chemical Engineering* **2021**, *9* (4), 105494. https://doi.org/10.1016/j.jece.2021.105494.
(21) Amiri, H.; Karimi, K. Pretreatment and Hydrolysis of Lignocellulosic Wastes for Butanol Production: Challenges and Perspectives. *Bioresource Technology* **2018**, *270*, 702–721. https://doi.org/10.1016/j.biortech.2018.08.117.
(22) Zeng, Z. K.; Jang, J. C.; Shurson, G. C.; Thakral, S.; Urriola, P. E. Ammonia Fiber Expansion Increases in Vitro Digestibility and Fermentability of Corn Distillers Dried Grains with Solubles with or without Carbohydrases. *Animal Feed Science and Technology* **2021**, *273*, 114824. https://doi.org/10.1016/j.anifeedsci.2021.114824.
(23) Knudsen, K. E. B. Fiber and Nonstarch Polysaccharide Content and Variation in Common Crops Used in Broiler Diets. *Poultry Science* **2014**, *93* (9), 2380–2393. https://doi.org/10.3382/ps.2014-03902.
(24) Zaini, N. A. B. M.; Chatzifragkou, A.; Charalampopoulos, D. Alkaline Fractionation and Enzymatic Saccharification of Wheat Dried Distillers Grains with Solubles (DDGS). *Food and Bioproducts Processing* **2019**, *118*, 103–113. https://doi.org/10.1016/j.fbp.2019.09.006.
(25) Mrudula Vasudevan, U.; Jaiswal, A. K.; Krishna, S.; Pandey, A. Thermostable Phytase in Feed and Fuel Industries. *Bioresource Technology* **2019**, *278*, 400–407. https://doi.org/10.1016/j.biortech.2019.01.065.
(26) Sharma, S.; Pradhan, R.; Manickavasagan, A.; Thimmanagari, M.; Saha, D.; Singh, S. S.; Dutta, A. Production of Antioxidative Protein Hydrolysates from Corn Distillers Solubles: Process Optimization, Antioxidant Activity Evaluation, and Peptide Analysis. *Industrial Crops and Products* **2022**, *184*, 115107. https://doi.org/10.1016/j.indcrop.2022.115107.
(27) Böttger, C.; Südekum, K.-H. Review: Protein Value of Distillers Dried Grains with Solubles (DDGS) in Animal Nutrition as Affected by the Ethanol Production Process. *Animal Feed Science and Technology* **2018**, *244*, 11–17. https://doi.org/10.1016/j.anifeedsci.2018.07.018.
(28) Li, X.; Cui, H.; Qiao, J.; Wang, M.; Yue, G. An Integrative Approach Enables High Bioresource Utilization and Bioethanol Production from Whole Stillage. *Bioresource Technology* **2022**, *343*, 126153. https://doi.org/10.1016/j.biortech.2021.126153.
(29) Pedersen, M. B.; Dalsgaard, S.; Knudsen, K. E. B.; Yu, S.; Lærke, H. N. Compositional Profile and Variation of Distillers Dried Grains with Solubles from Various Origins with Focus on Non-Starch Polysaccharides. *Animal Feed Science and Technology* **2014**, *197*, 130–141. https://doi.org/10.1016/j.anifeedsci.2014.07.011.
(30) Lee, J.; Nam, D. S.; Kong, C. Variability in Nutrient Composition of Cereal Grains from Different Origins. *SpringerPlus* **2016**, *5* (1), 419. https://doi.org/10.1186/s40064-016-2046-3.
(31) Liu, K. Chemical Composition of Distillers Grains, a Review. *J. Agric. Food Chem.* **2011**, *59* (5), 1508–1526. https://doi.org/10.1021/jf103512z.
(32) Böttger, C.; Südekum, K.-H. Within Plant Variation of Distillers Dried Grains with Solubles (DDGS) Produced from Multiple Raw Materials in Varying Proportions: Chemical Composition and in Vitro Evaluation of Feeding Value for Ruminants. *Animal Feed Science and Technology* **2017**, *229*, 79–90. https://doi.org/10.1016/j.anifeedsci.2017.05.003.
(33) Novozymes A/S. *Liquefaction*; 2022.
(34) Kurambhatti, C.; Kumar, D.; Rausch, K.; Tumbleson, M.; Singh, V. Ethanol Production from Corn Fiber Separated after Liquefaction in the Dry Grind Process. *Energies* **2018**, *11* (11), 2921. https://doi.org/10.3390/en11112921.

(35) B. Hames; R. Ruiz; C. Scarlata; A. Sluiter; J. Sluiter; D. Templeton. *Preparation of Samples for Compositional Analysis*; Laboratory Analytical Procedure (LAP); Technical Report NREL/TP-510-42620; National Renewable Energy Laboratory: Golden, Colorado, 2008.
(36) A. Sluiter; B. Hames; R. Ruiz; C. Scarlata; J. Sluiter; D. Templeton. *Determination of Ash in Biomass*; Laboratory Analytical Procedure (LAP); Technical Report NREL/TP-510-42622; National Renewable Energy Laboratory: Golden, Colorado, 2008.
(37) Technical, A. Crude Protein--Combustion Method. In *AACC International Approved Methods*; AACC International, 2009. https://doi.org/10.1094/AACCIntMethod-46-30.01.
(38) A. Sluiter; R. Ruiz; C. Scarlata; J. Sluiter; D. Templeton. *Determination of Extractives in Biomass*; Laboratory Analytical Procedure (LAP); Technical Report NREL/TP-510-42625; National Renewable Energy Laboratory: Golden, Colorado, 2008.
(39) A. Sluiter; B. Hames; R. Ruiz; C. Scarlata; J. Sluiter; D. Templeton; D. Crocker. *Determination of Structural Carbohydrates and Lignin in Biomass*; Laboratory Analytical Procedure (LAP); Technical Report NREL/TP-510-42618; National Renewable Energy Laboratory: Golden, Colorado, 2012.
(40) Corassa, A.; Gonçalves, D. B. C.; Freitas, L. W. de; Kiefer, C.; Straub, I. W. W.; Rothmund, V. L.; Saucedo, K. M. B.; Correa, D. Variabilidade Da Composição Nutricional de Coprodutos de Etanol de Milho Do Brasil Para Suínos. *RSD* **2021**, *10* (13), e105101321031. https://doi.org/10.33448/rsd-v10i13.21031.
(41) Kim, D.; Orrego, D.; Ximenes, E. A.; Ladisch, M. R. Cellulose Conversion of Corn Pericarp without Pretreatment. *Bioresource Technology* **2017**, *245*, 511–517. https://doi.org/10.1016/j.biortech.2017.08.156.
(42) Knudsen, K. E. B. Carbohydrate and Lignin Contents of Plant Materials Used in Animal Feeding. *Animal Feed Science and Technology* **1997**, *67* (4), 319–338. https://doi.org/10.1016/S0377-8401(97)00009-6.
(43) Shurson, G. C. Yeast and Yeast Derivatives in Feed Additives and Ingredients: Sources, Characteristics, Animal Responses, and Quantification Methods. *Animal Feed Science and Technology* **2018**, *235*, 60–76. https://doi.org/10.1016/j.anifeedsci.2017.11.010.
(44) Cabib, E.; Roberts, R.; Bowers, B. Synthesis of the Yeast Cell Wall and Its Regulation. *Annu. Rev. Biochem.* **1982**, *51* (1), 763–793. https://doi.org/10.1146/annurev.bi.51.070182.003555.
(45) Kollár, R.; Petráková, E.; Ashwell, G.; Robbins, P. W.; Cabib, E. Architecture of the Yeast Cell Wall. *Journal of Biological Chemistry* **1995**, *270* (3), 1170–1178. https://doi.org/10.1074/jbc.270.3.1170.
(46) Kapteyn, J. C.; Montijin, R. C.; Vink, E.; de la Cruz, J.; Llobell, A.; Douwes, J. E.; Shimoi, H.; Lipke, P. N.; Klis, F. M. Retention of *Saccharomyces Cerevisiae* Cell Wall Proteins through a Phosphodiester-Linked β -1,3-/ β -l,6-Glucan Heteropolymer. *Glycobiology* **1996**, *6* (3), 337–345. https://doi.org/10.1093/glycob/6.3.337.
(47) Han, J.; Liu, K. Changes in Composition and Amino Acid Profile during Dry Grind Ethanol Processing from Corn and Estimation of Yeast Contribution toward DDGS Proteins. *J. Agric. Food Chem.* **2010**, *58* (6), 3430–3437. https://doi.org/10.1021/jf9034833.
(48) Novozymes A/S. *Novozymes Cellic® CTec3 HS - Secure Your Plant's Lowest Cost*; Application sheet; 2017; p 6.
(49) Novozymes A/S. *Get the Most from Your Corn and All Your Mills with Novozymes Frontia® Fiberwash*; 2018; p 2.
(50) Novozymes A/S. *VinoTaste® Pro Product Data Sheet*; 2017; p 2.
(51) Appeldoorn, M. M.; Kabel, M. A.; Van Eylen, D.; Gruppen, H.; Schols, H. A. Characterization of Oligomeric Xylan Structures from Corn Fiber Resistant to Pretreatment and Simultaneous Saccharification and Fermentation. *J. Agric. Food Chem.* **2010**, *58* (21), 11294–11301. https://doi.org/10.1021/jf102849x.

(52) Jonathan, M. C.; DeMartini, J.; Van Stigt Thans, S.; Hommes, R.; Kabel, M. A. Characterisation of Non-Degraded Oligosaccharides in Enzymatically Hydrolysed and Fermented, Dilute Ammonia-Pretreated Corn Stover for Ethanol Production. *Biotechnol Biofuels* **2017**, *10* (1), 112. https://doi.org/10.1186/s13068-017-0803-3.

(53) Appeldoorn, M. M.; de Waard, P.; Kabel, M. A.; Gruppen, H.; Schols, H. A. Enzyme Resistant Feruloylated Xylooligomer Analogues from Thermochemically Treated Corn Fiber Contain Large Side Chains, Ethyl Glycosides and Novel Sites of Acetylation. *Carbohydrate Research* **2013**, *381*, 33–42. https://doi.org/10.1016/j.carres.2013.08.024.

(54) Zhang, L.; Jin, Y.; Xie, Y.; Wu, X.; Wu, T. Releasing Polysaccharide and Protein from Yeast Cells by Ultrasound: Selectivity and Effects of Processing Parameters. *Ultrasonics Sonochemistry* **2014**, *21* (2), 576–581. https://doi.org/10.1016/j.ultsonch.2013.10.016.

(55) Rose, D. J.; Inglett, G. E. A Method for the Determination of Soluble Arabinoxylan Released from Insoluble Substrates by Xylanases. *Food Anal. Methods* **2011**, *4* (1), 66–72. https://doi.org/10.1007/s12161-009-9121-0.

(56) Dien, B. S.; Ximenes, E. A.; O'Bryan, P. J.; Moniruzzaman, M.; Li, X.-L.; Balan, V.; Dale, B.; Cotta, M. A. Enzyme Characterization for Hydrolysis of AFEX and Liquid Hot-Water Pretreated Distillers' Grains and Their Conversion to Ethanol. *Bioresource Technology* **2008**, *99* (12), 5216–5225. https://doi.org/10.1016/j.biortech.2007.09.030.